Helene Thekkekara Puthenparampil, BSc

Validation of circRNAs and their expression during mouse brain development and neuronal maturation

MASTER'S THESIS

to achieve the university degree of

Master of Science

Master's degree program: Molecular Microbiology

submitted to

Graz University of Technology

Supervisors

Dr. Roel Quintens

SCK•CEN - Belgian Nuclear Research Centre

Univ.-Prof. Dr. Kai-Uwe Fröhlich

Institute of Molecular Biosciences, University of Graz

Graz, June, 2016

AFFIDAVIT

I declare that I have authored this thesis independently, that I have not used other than the declared sources/resources, and that I have explicitly indicated all material which has been quoted either literally or by content from the sources used. The text document uploaded to TUGRAZonline is identical to the present master‘s thesis dissertation.

_____	_____
Date	Signature

Acknowledgements

I take this opportunity to extend my heartfelt thanks to all those who have contributed to make this master thesis a success. First and foremost, I would like to thank my mentor at SCK·CEN, Dr. Roel Quintens, for his dedicated involvement and incredible support during the practical and theoretical work of my thesis. He has invested immense amount of time and effort teaching me all the different techniques at lab, patiently explaining and discussing different theoretical matters while never failing to encourage me during each step of my way.

I would also like to thank my supervisor at my university, Univ.-Prof. Dr. Kai-Uwe Fröhlich, for his always encouraging words and cheerful smiles. He has always welcomed me with open hands whenever I needed help with organizational matters and a plethora of various questions.

I am very grateful to all my colleagues at SCK·CEN who have offered me a very pleasant working environment, to Dr. Sarah Baatout for accepting me and allowing me to complete the internship and to SCK·CEN itself for having me.

Thank you very much André Claude Mbouombouo Mfossa for welcoming me to the group and being there for me from day one of my internship. A special thank you also to Ann Janssen, who has always helped me out whenever I felt completely lost in the labs.

I am very grateful to Mieke Neefs, Jasmine Buset and Akshaya Ramakrishnan for all the help with the cell cultures and computational work. I would like to express my special gratitude to Dr. Mieke Verslegers, Dr. Rafi Benotmane and Mohamed Ahmed for sharing their pearls of wisdom with me and helping me with great pieces of advice whenever I needed them.

A special gratitude goes to my beloved family and friends for all the support they have given me. Thank you to my beloved husband and my lovely parents for the continuous encouragement, endurance and the unfailing support they have offered me throughout my years of study and through the process of researching and writing this thesis. This accomplishment would not have been possible without them.

Finally, and most importantly, I would like to extend my sincere thanks to God, the Almighty, who has always given me courage and held my hands through the most difficult times, not only during the process of writing this thesis, but throughout my entire life. Thank you!

Abstract

Circular RNAs (circRNAs) are a new type of mostly non-coding RNA species that unlike linear RNAs form covalently closed, continuous loops and have recently been shown to be highly abundant, evolutionarily conserved and relatively stable in the cytoplasm[1]. circRNAs that are formed by backsplicing events can consist of one or more exonic and/or intronic sequences and are mainly involved in gene regulating processes. The key-function of the circRNAs that has been proven until now is their activity as miRNA-sponges[2, 3, 7]. Genome-wide screenings of circRNA expression have shown that they are enriched in the mammalian brain, and dynamically expressed during *in vitro* neuronal differentiation and *in vivo* brain development[1].

Strikingly, we noticed similar features also in the radiation-responsive genes that had been identified in a previous study done in embryonic mouse brains. These radiation-responsive genes are also generally highly induced during *in vivo* brain development and *in vitro* neuronal differentiation[4], and most intriguingly, we learned that many of these genes are predicted to express circRNAs. In this study, we aimed at validating the expression of the circular isoforms of two of those genes, *Pvt1* and *Ano3*, and at the characterization of their expression profiles in comparison to their cognate linear mRNAs. We successfully validated the expression of stable circRNAs for both *Pvt1* and *Ano3*, and found them to be enriched in the mouse brain. Moreover, we observed an induction of the circular transcripts (of both genes) during neuronal maturation and brain development, and found very first indications of radiation-responsive circRNAs. Based on our results, we suspect that the circular transcripts in particular may be deeply involved in brain development related matters. The deviating and dynamically regulated expression profiles of the circRNAs from their cognate mRNAs in any case suggest that they play a unique and significant role in cellular functioning.

Kurzzusammenfassung

Zirkuläre RNAs (circRNAs) gehören zu einer neuen, meist nicht-kodierenden Gruppe von RNAs, die im Gegensatz zu den linearen mRNAs einen kovalent geschlossenen Ring bilden. circRNAs entstehen durch die Zirkularisierung von einen oder mehreren Exonen und/oder Intronen und sind abundant, evolutionär konserviert und relativ stabil im Zytoplasma[1]. Vermutlich spielen die circRNAs eine große Rolle in der Genregulation. Ihre bisher nachgewiesene Hauptfunktion besteht in ihrer Aktivität als Regulator der miRNAs[2, 3, 7]. Genomweit durchgeführte Studien haben gezeigt, dass die circRNAs nicht nur angereichert sind im Gehirn der Säugetiere, sondern auch dynamisch exprimiert sind in der *in vitro* neuronalen Differenzierung und der *in vivo* Hirnentwicklung[1].

In einer früheren Studie in embryonalen Mäusen hatte man eine Gensignatur identifiziert, die bei ionisierender Bestrahlung aktiviert werden. Interessanterweise haben wir entdeckt, dass die Expression dieser Gene, ähnlich wie die der circRNAs, auch hinaufreguliert sind während der Hirnentwicklung und der neuronalen Differenzierung[4]. Vor allem stellte sich heraus, dass viele der Gene aus dieser Gensignatur, nach Voraussagen durch algorithmische Kalkulierungen, vermutlich ebenfalls zirkuläre Isoformen exprimieren.

Das Ziel dieser Arbeit ist die Überprüfung und Validierung der Expression der vorausgesagten zirkulären RNAs für zwei ausgesuchte Gene aus der Signatur, *Pvt1* und *Ano3*, und die Charakterisierung ihrer Expressionsprofile im Vergleich zu ihren linearen Isoformen. Uns ist es gelungen für beide Gene, *Pvt1* und *Ano3*, circRNA-Expression nachzuweisen. Eine Anreicherung dieser circRNAs im Gehirn der Mäuse wurde festgestellt. Außerdem beobachteten wir eine Induktion dieser circRNAs in der neuronalen Reifung (*in vitro)* und während der Hirnentwicklung (*in vivo*). Ebenfalls beobachteten wir einige erste Hinweise auf circRNAs, die auf Strahlung reagieren. Basierend auf unseren Ergebnissen vermuten wir, dass die circRNAs eventuell eine besonders signifikante Rolle spielen in der Gehirnentwicklung. Die von der linearen Isoform abweichenden und dynamisch-geregelten Expressionsprofile der circRNAs legen in jeden Fall nahe, dass die zirkulären Transkripte einzigartige und wichtige zelluläre Funktionen haben.

Table of contents

1. Introduction

1.1. A brief overview of the human brain

The human brain, the main organ of the nervous system, can be considered the most complex organ among all biological systems[5]. It is composed out of neurons, the information processing cells, glial cells, mainly astrocytes and oligodendrocytes, which are the "supporting cells" and blood vessels. An average mature human brain weighs 1.3 – 1.4 kg and has a characteristic pattern of folds (sulci) and ridges (gyri) [5, 6].

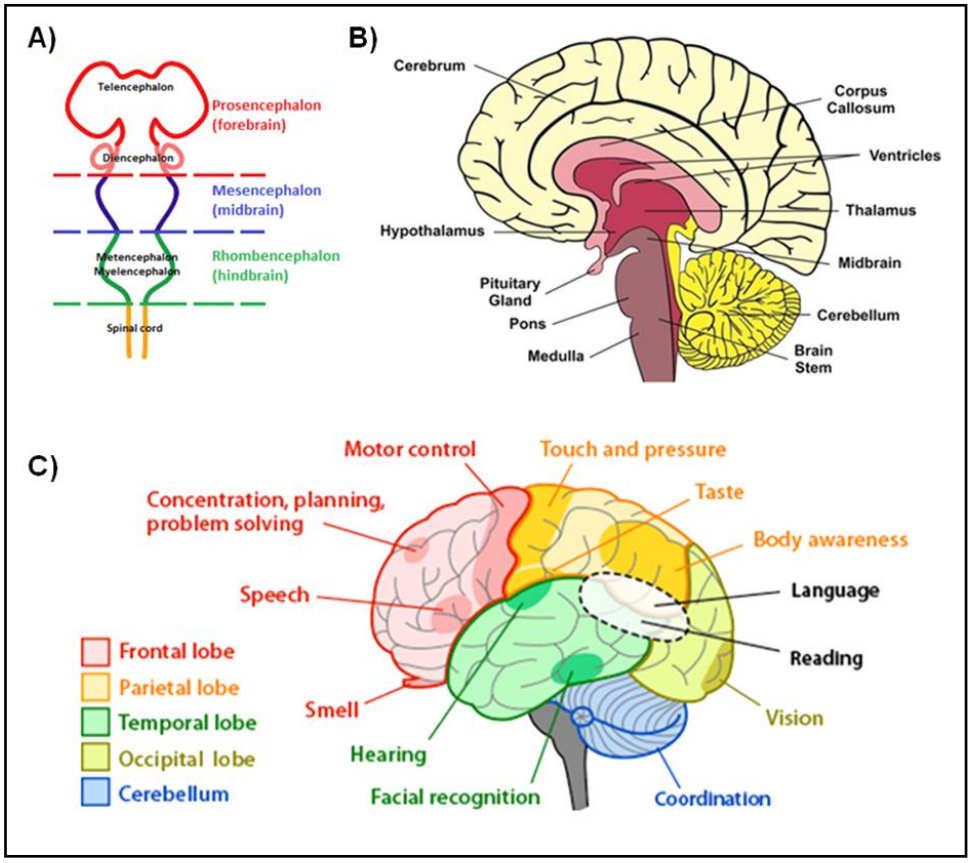

Figure 1. Anatomy of the human brain. (**A**) The main subdivisions of the embryonic vertebrate brain are depicted in this diagram. (**B**) One representation of the anatomical regions of the human brain that is composed of many different regions is given here. (**C**) The brain can be divided into different lobes that are dedicated to different functions in the body. This illustration shows a rough spatial map with the lobes and their functions. Adapted from [8, 9, 108].

The largest and most important parts of the information processing system are the neocortex that accounts for most of the cerebral cortex and the subcortical nuclei that relay information from and to the neocortex. The greyish appearance due to the high content of cell bodies in these structures is the reason why these components are referred to as the "grey matter". The neurons are connected to one another by fibers that extend from cell bodies of individual neurons, such as dendrites and axons. Some axons are surrounded by a fatty substance called myelin, which is an electrically insulating layer that improves the transmission of electrical signals between regions. The myelin sheets are produced by oligodendrocytes, and

regions of the brain rich in myelinated axons appear white, giving rise to the term "white matter"[5].

There are four interconnected cavities at the very center of the brain that are filled with the cerebral spinal fluid, forming the ventricular system. Some of the important functions of this system are cushioning and protection of the brain, removal of waste material and transport of other substances, such as hormones[5].

Our brain can be divided into many areas that are structurally different and are specialized for carrying out different kinds of processes[5]. Basically, the embryonic vertebrate brain can be divided into three main parts: the forebrain, midbrain and hindbrain (**Figure 1 A**). During early development of the central nervous system, the forebrain separates into the diencephalon, which consists of the thalamus, hypothalamus, subthalamus, epithalamus and pretectum, and the telencephalon, which develops into the cerebrum (**Figure 1 A, B**). The cerebrum is the largest part of the brain and is divided into two cerebral hemispheres and is connected by the corpus callosum. The cerebral cortex, cerebrum's outer layer of neural tissue is divided into four lobes; the frontal, parietal, temporal and occipital lobes. The midbrain mainly consists of the tectum, tegmentum, the cerebral aqueduct and the cerebral peduncles. The hindbrain mainly consists of the cerebellum, pons and medulla oblongata[6, 108, 117]. Each of these structures is responsible for a number of different functions (**Figure 1 C**).

1.1.1. Brain Development

The development of the brain consists of a very complex and strictly regulated sequence of events (**Figure 2**) during which a variety of specialized neural and non-neural cell types are produced. An adequate timely switching of the different developmental stages is critical for proper neural circuit formation and normal brain function[10].

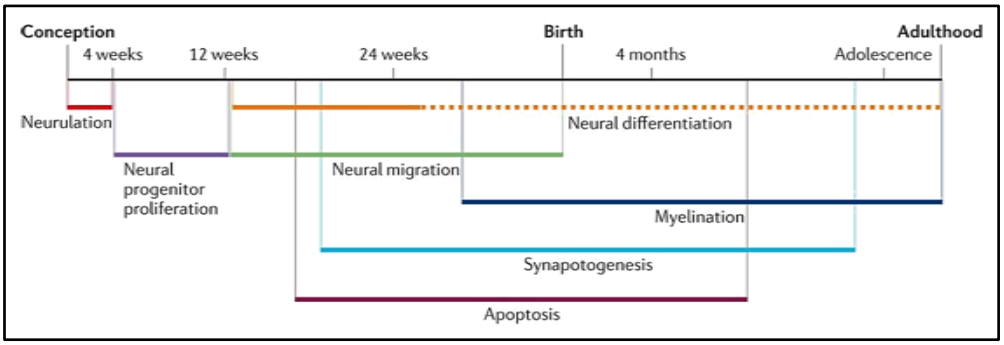

Figure 2. Timeline: Development of the human brain. The key events of human brain development are represented in a timeline that stretches from conception to adulthood. Adopted from [11].

The nervous system is derived from the ectoderm, the most exterior germ layer in the very early embryo. As a result of different signaling events, the neuroectoderm, which develops from the ectoderm, is transformed into the neural plate, neural groove and finally the neural tube, the first brain structure[5, 12]. The neuroepithelial cells, the neural progenitors, are located

at the ventricular zone, in the region of the neural tube adjacent to the cavity. In the embryo, this cavity formed by neurulation is cylindrical, but changes its shape gradually to eventually form the ventricular system[5, 13]. This event is followed by massive cell proliferation, and once the neurons are formed, the neuronal migration starts. While reaching their final destinations, environmental changes steer them toward final differentiation[14].

Maturation of the different cell types, synaptogenesis (the formation of interneuronal connections), and myelination are the final events that follow and continue taking place for an extended period after birth (**Figure 2**). The brain expands in size, complexity and surface area gradually leading to the mature gyrencephalic structure of the adult human brain. On average, the human brain takes 20 – 25 years to fully mature[10], although new neurons are continuously produced and integrated throughout life[15].

1.1.2. Development of the neocortex

The neocortex is the most developed part of the cerebral cortex and is involved in functions such as sensory perception, generation of motor commands, spatial reasoning, conscious thought and language[16]. The size and surface area of the neocortex are thought to be critical factors that influence a species' cognitive abilities and sensorimotor skills. Disruption of neocortical structures and folding are the key reasons for many neurological disorders[17]. The neocortex is made up of six horizontal cellular layers, each consisting of a unique subset of neuronal population establishing local and long-range connections[16].

Neurons of the cerebral cortex arise in the germinal ventricular zone at the surface of the lateral ventricles. The timely strictly coordinated assembly of the cortex (**Figure 3A**) to the six-layered cortical structure (**Figure 3D**) is accomplished by the radial progenitors that are derived from the neuroepithelial cells and consist of proliferative radial glial cells and their more differentiated daughter cells that include neurons, astrocytes and oligodendrocytes[18].

Radial glia undergo both symmetrical divisions to self-renew and asymmetrical neurogenic divisions. During neurogenesis, mainly asymmetrical divisions occur, giving rise to one radial glial cell and a post-mitotic neuron or an intermediate progenitor, of which two types exist: apical intermediate progenitors that reside in the ventricular zone and have short radial attachment to the ventricular surface, and basal intermediate progenitors that migrate into the subventricular zone. Intermediate progenitors usually undergo one to two proliferative divisions before dividing asymmetrically to two post-mitotic neurons[18]. The radial glial cells can also be divided into the classical bipolar ventricular surface-attached apical radial glial cells and to the more recently identified basal radial glial cells that are unipolar, but behave similarly (**Figure 3C**)[17].

Interestingly, interkinetic nuclear migration, an oscillation process of the nuclei of the progenitor cells in coordination with the cellcycle, is a common feature of developing neuroepithelia. During S-phase the nuclei of ventricular zone progenitors are situated at the basal side of the ventricular zone, but move towards the apical surface during G2 phase,

where they undergo mitosis and return to the basal position in the G1 phase (**Figure 3B**)[19]. Recent experiments in mouse embryos have clearly shown that prenatal radiation exposure results in a transient and dose-dependent G2/M arrest of radial glia[20].

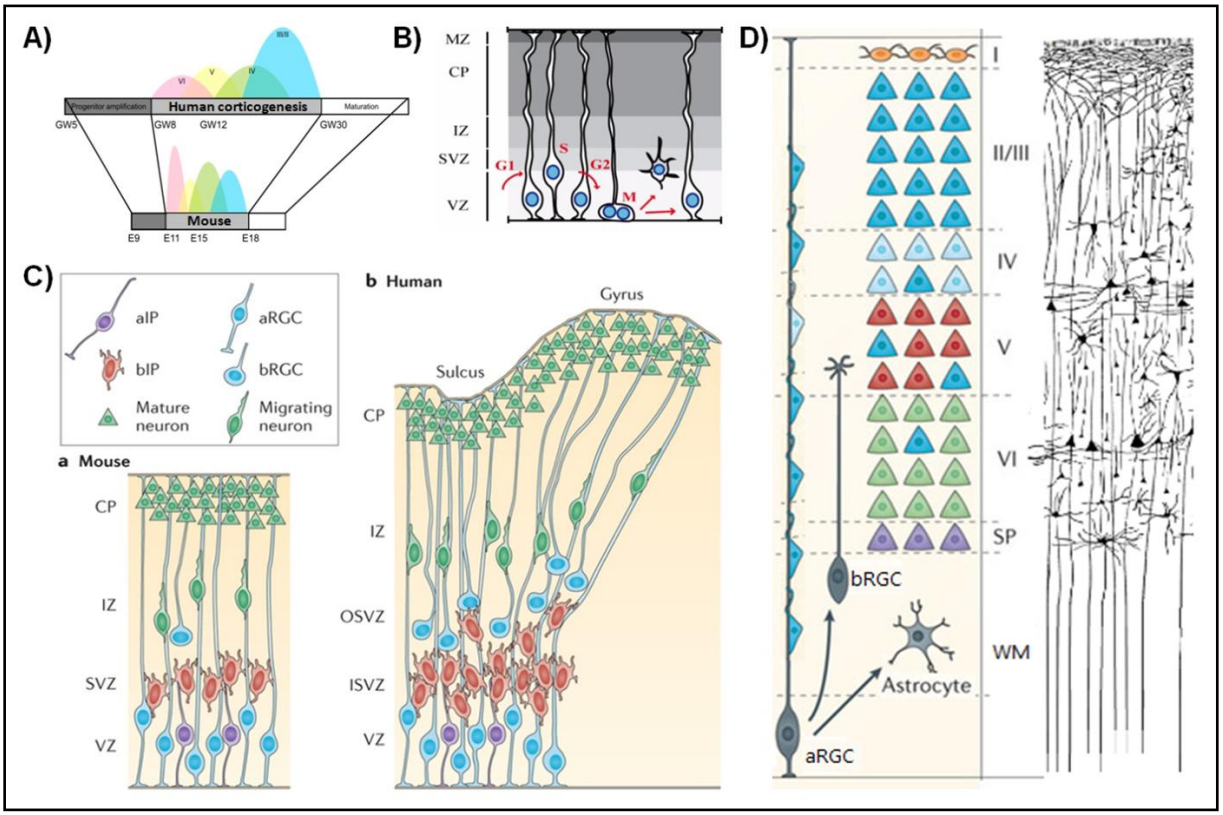

Figure 3. The developing cerebral cortex and the interkinetic nuclear migration. (**A**) Chronology of development of the different layers of the neocortex in humans and mice. Human corticogenesis follows a more protracted time-course than the mouse. (**B**) The oscillation process of the radial glia nuclei (interkinetic nuclear migration) that is dependent on the cell cycle. (**C**) The sketch shows the position of the neural progenitors and migrating neurons in the developing cortex of mice (**a**) and humans (**b**). aIP: apical intermediate progenitors; aRGC: apical radial glial cells; bIP: basal intermediate progenitors; bRGC: basal radial glial cells; CP: cortical plate; ISVZ: inner SVZ; IZ: intermediate zone; MZ: marginal zone; OSVZ: outer SVZ; SP: subplate; SVZ: subventricular zone; VZ: ventricular zone; WM: white matter. (**D**) The histological structure of the cerebral cortex showing its six layers. Adapted from [17, 21-25].

Neurons use different strategies, such as radial or tangential migration, to travel from their origin to their final positions in the brain where they mature and fulfill their destiny. Most neurons produced in the ventricular zone migrate radially from inner to outer zones with the help of radial glia that form a connection between the inner and outer edges (radial fibers) serving as a scaffold for migrating neurons (**Figure 4**)[5, 17]. During tangential migration, so-called interneurons move parallel to the ventricular surface[26]. A balanced proliferation, differentiation and migration of the different progenitor cells are crucial for the proper development of the cortex[17].

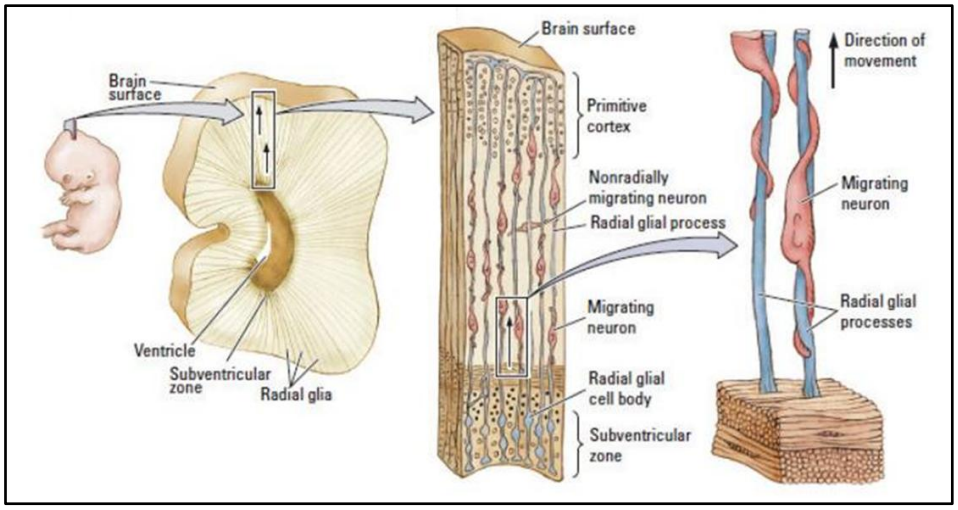

Figure 4. Radial migration of neurons along the radial glia from the subventricular zone to the outer cortical layers. This figure illustrates the glia-guided migration process of the cortical neurons, zoomed-in in three steps. Adopted from [14].

1.2. Ionizing Radiation

The emission of energy from a source as electromagnetic waves (**Figure 5**) or particles is generally referred to as radiation. Depending on the energy level of the radiated particle or wave, radiation is often classified as non-ionizing and ionizing radiation[27]. If the radiation has sufficient energy to remove one or more orbital electrons from an atom or molecule, creating charged atoms/molecules, the process is called ionization, and the radiation is then characterized as ionizing radiation[28]. The emission of ionizing radiation can happen either in the decay process of unstable nuclei or by de-excitation of atoms and their nuclei[29].

Non-ionizing, low-frequency radiation that includes visible light, microwaves, radio waves and partly the ultraviolet waves, disperses energy through heat and increased molecular movements. This type of radiation is in general not considered significantly risky since it only leads to problems related to excessive heating when exposed to high intensities. In contrast, Gamma rays, X-rays and the higher ultraviolet part of the electromagnetic spectrum (**Figure 5**) as well as alpha- and beta-particles belong to ionizing radiation that emits high energy waves or particles, possibly causing significant risks to organisms by altering the structure and behavior of cells[30].

Ionizing radiation itself can be subdivided into low linear energy transfer (LET) radiation, such as X- and gamma rays, and high LET radiation like that of charged particles. LET describes the amount of energy an ionizing particle transfers to the material traversed per unit distance and its unit is keV/µm[29, 31].

Alpha radiation consists of positively charged helium nuclei. These particles are heavy, interact quickly with materials they encounter and travel no more than a few inches in air. They can be shielded by a sheet of paper or the epidermis[32]. It is therefore not an external

hazard, though alpha-emitting materials can be harmful to humans when the body is internally contaminated. Radon and uranium are good examples of alpha emitters[33, 34].

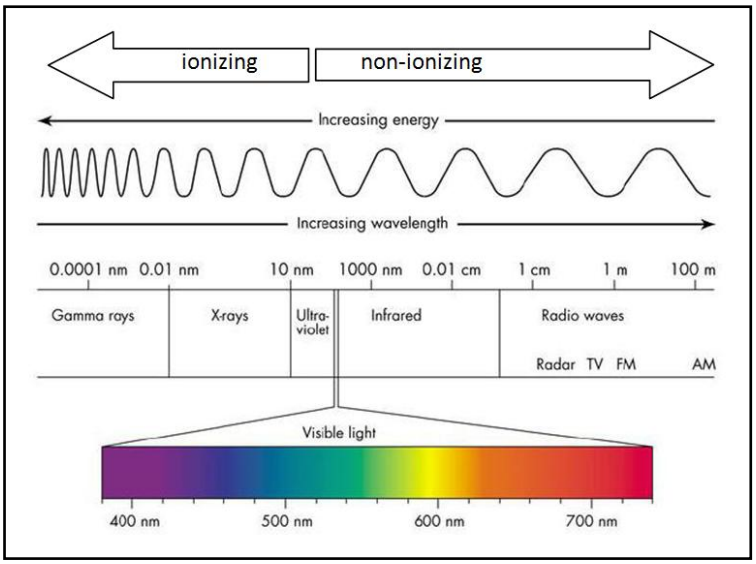

Figure 5. The electromagnetic spectrum. Gamma rays, X-rays and the high-energy part of ultra-violet radiation are considered ionizing, while visible light, infrared, radio waves and the low-energy part of ultra-violet radiation are considered non-ionizing radiation. The energy of the respective radiation is proportional to its frequency and inversely related to its wavelength. Adapted from [35].

Beta radiation that consists of ejected electrons is a light, short-range particle that is moderately penetrating and can be stopped by an aluminium plate. Similar to alpha radiation, beta radiation can also cause severe damage if deposited internally in the body. Common examples for beta emitters are strontium-90 and tritium[33, 34].

Gamma radiation and X-rays are highly penetrating electromagnetic radiations that have neither mass nor electric charge. Dense materials like thick layers of concrete and lead are required to stop them[33, 34]. Gamma radiation and X-rays mainly differ from each other by the way they are produced. Gamma radiation, which is positioned higher in the electromagnetic spectrum than X-ray due to its higher energy level, originates from the nucleus of a radionuclide after radioactive decay. X-rays on the other hand are produced when the electrons collide with atoms and nuclei of a target or when electrons are rearranged within an atom[13]. Radioactive materials that emit gamma radiation and X-rays, like iodine-131 or radium-226, pose both external and internal hazards to humans[34].

1.2.1. Sources and applications of ionizing radiation

Every human being is constantly exposed to a certain dose of radiation in their daily lives. There are naturally occurring environmental sources of radiation and also man-made radiation from industrial, occupational and medical sources that pose a possible risk to human health. Natural radiation for humans comes from the sun, cosmic rays and the naturally-occurring radioactive elements in the earth's crust, such as uranium, thorium and

their decay products like radium and radon. Man-made radiation is produced in devices, such as X-ray machines or in reactors or accelerators that produce artificial radioisotopes[36].

Despite the hazardous nature, ionizing radiation is generated and utilized in a wide variety of applications in various fields. Medical facilities, such as hospitals and pharmaceutical facilities, research and teaching institutions, nuclear reactors and their supporting facilities, such as uranium mills, are only examples where radiation finds great usage. Also some consumer products such as smoke detectors and self illuminating exit signs make use of radioactive materials[36]. The usage of radiation in the medical field for therapeutic and diagnostic procedures has risen immensely during the past decade, and this trend keeps increasing. **Table 1** provides an overview of some common medical applications of radiation[30].

The gray (Gy) is the unit for the absorbed dose of ionizing radiation, defined as the absorption of radiation energy per unit mass of tissue. The sievert (Sv) is the unit of equivalent dose for biological damage[37, 38]. If gray is a physical quantity or the amount of energy that is deposited in the human tissue, sievert represents the equivalent biological effect of the deposit of a joule of radiation energy in a kilogram of human tissue[39].

Type of radiation	Medical application
Ionizing radiation:	
Gamma Rays	PET
	RT
	SPECT
X-rays	CT
	DSA
	Dual-energy X-ray absorptiometry
	Fluoroscopy
	Mammography
	RT
	Radiography
Non-ionizing radiation:	
Electromagnetic and RF waves	MRI
Ultrasound	US

Table 1. Common medical applications of non-ionizing and ionizing radiation. CT: computed tomography; DSA: digital subtraction angiography; MRI: magnetic resonance imaging; PET: positron emission tomography; RT: radiation therapy; RF: radiofrequency; SPECT: single-photon emission computed tomography; US: ultrasonography. Adapted from [30].

The total exposure of an average adult to ionizing radiation is approximately 3 mSv per year. Around half of that amount comes from medical procedures where radiation is used for diagnostic and therapeutic purposes. The chart below (**Figure 6**) gives an overview of the distribution of radiation sources that amount for our average annual exposure[40].

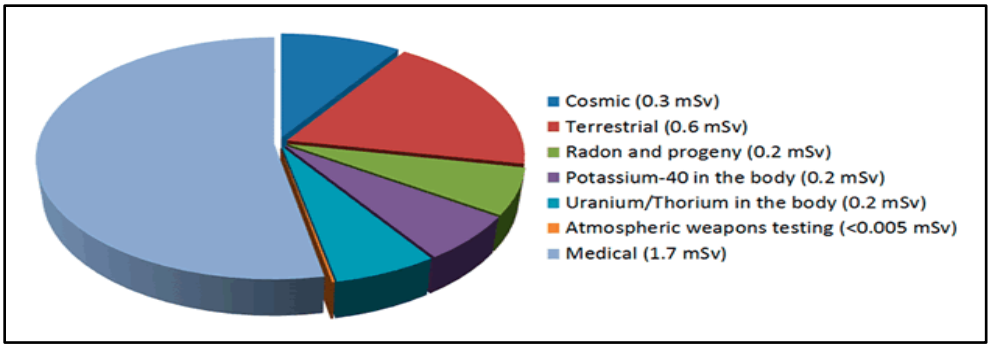

Figure 6. Average annual exposure to radiation. Representative for the western countries, this chart illustrates the distribution of radiation sources that amount for the average annual exposure to radiation of an adult in Australia. More than half the amount of radiation exposure is due to medical applications of radiation. Adopted from [40].

1.3. Radiation and the human body

Most of our knowledge about the consequences of radiation, its teratogenic, carcinogenic and mutagenic effects in the body, comes from studies performed after well known acute exposures, such as the atomic bombings in Japan 1945 or the Chernobyl accident in 1986[28].

Besides its most eminent cancerous effects, there exist a variety of other health risks that may follow exposure to ionizing radiation (**Table 2**). Cardiovascular diseases, strokes, cortical cataract, non-malignant respiratory and digestive diseases, reductions of intelligence quotient and increase in incidents of severe mental retardation are examples for such non-cancerous consequences[41, 77].

The biological effects of radiation on the human body can be classified into two major categories: deterministic and stochastic effects. Deterministic effects are caused by exposure to high doses of radiation and the damage depends on the absorbed dose of irradiation. Cataract, erythema, and infertility are examples of predictable deterministic effects of radiation that are caused by multi-cellular injuries and chromosome aberrations. For these, there is a threshold below which there is no effect to be observed and the threshold level is dependent on the effect, tissue and individual (**Table 2**). Stochastic effects are independent of the absorbed dose; there is no threshold dose. Any dose could result in stochastic effects, such as life span shortening, cancer and other genetic effects due to germ cell mutations. The probability of occurrence rises as dose increases, but the severity of the stochastic effect is not dose-related[42].

Effect	Dose, Sv	References
Acute radiation syndromes		
Nausea and vomiting	0.5 acute	Young et al. 1987
Early skin reaction	0.5-1 acute	Conklin and Walker 1987
Late skin reaction	5-10 acute	ICRP 1991
Gastrointestinal syndrome	~7 acute	Young et al. 1987
CNS syndrome	~50 acute	Young et al. 1987
Cataracts		
Detectable opacities (recent emerging data)	0.5 acute, 5 fractionated < 0.8 (?) acute & chronic	ICRP 1991 Neriishi et al. 2007 Worgul et al. 2007 Chylack et al. 2009 Blakely et al. 2010
Vision impairing opacities	5 acute, > 8 fractionated	ICRP 1991
Central nervous system		
Adult (cognition)	< 30 fractioned < 5 acute	Chang et al. 2009 CCMDC 1981
In utero (severe mental retardation)	~0.15 acute	Otake et al. 1987
In utero (reduction in IQ)	~0.1 acute	Schull et al. 1988 ICRP 1991
Malformations in fetus	~0.1 acute	ICRP 1991
Cardiovascular	~0.5 acute	Preston et al. 2003
Fertility		
Man temporary infertility	0.15 acute 0.4 Sv/year chronic	NRC 1990 ICRP 1991
Man permanent sterility	3 acute, 5 fractionated 2 Sv/year chronic	UNSCEAR 1982 ICRP 1991
Woman temporary infertility	0.65 – 1.5 acute	ICRP 1984
Woman permanent sterility	2.5 acute, 6 fractionated > 2 Sv/year chronic	NCRP 1990
Woman premature menopause (if exposed *in utero*)	~0.5 (?) chronic	Straume et al. 2010

Table 2. Low-LET radiation and its estimated dose-dependent biological effects on the human body. Some deterministic effects with its estimated threshold levels are summarized here with indications to the respective studies they were published in. Adapted from [43].

1.3.1. Models predicting the risk from exposure to ionizing radiation

There exist several quantitative models for predicting the level of health risk from radiation exposure. A well established and routinely used model in radiation safety regulations and practices throughout the world is the linear no-threshold (LNT) dose-response relationship model[44], that puts the risks in direct and proportional relationship with radiation exposure[45], claiming that even the smallest dose may lead to biological effects[46]. The potential risk here is calculated by extrapolation from medium and higher doses. However, due to the difficulty to observe and interpret, health effects of low dose radiation have still not been completely characterized. Data indicate that cellular responses might differ at low compared to high doses[47], which is why the LNT model has become controversial. Some alternative hypotheses such as the threshold model suggest that there is no risk below a certain dose,

while the radiation hormesis model even claims that radiation at very small doses can be protective and beneficial (**Figure 7**). Nevertheless, in agreement with the LNT model, the ALARA principle urging to keep the exposure As Low As Reasonably Achievable, has become a fundamental approach when dealing with radiation[45].

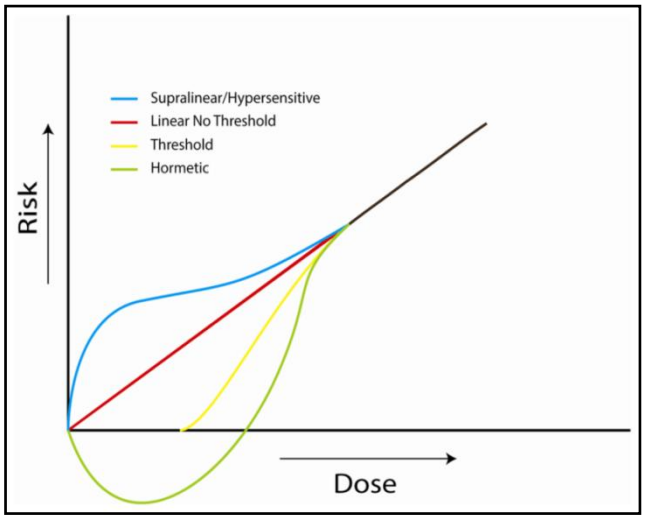

Figure 7. Radiation risk models. While the linear no-threshold model puts the risk and health effects in direct proportion, the hypersensitivity model suggests a greater risk at lower doses, and the threshold model only a risk from above a certain threshold level. The hormesis model claims a beneficial effect at lower radiation doses. Adopted from [48].

1.3.2. Cellular response to radiation

Ionizing radiation can cause high stress levels in cells, through the induction of cellular damage by direct ionization of macromolecules such as DNA, RNA, lipids and proteins or by indirect ionization leading to generation of free radicals, such as reactive oxygen or nitrogen species, which can in their turn target these macromolecules (**Figure 8**). High LET radiation mainly causes cell damage via direct interactions, while low LET radiation mostly leads to the production of free radicals. In any case, this can lead to the activation of several intracellular signaling pathways resulting in a stress response[49]. Since about 80% of a cell is composed of water, it is especially superoxide and hydroxyl radicals that are formed by radiolysis of intracellular water[50] (**Figure 8**). Nitrogenous base alterations, breaks in one or both DNA chains and chain cross-linking after breakage are examples for ionizing radiation-induced DNA damages, among which double strand breaks (DSBs) are considered the most harmful. Unrepaired DNA damage may lead to mutations, genomic instability and cell death[49]. Not only chromosomal DNA is affected, but also mitochondrial DNA, maybe even to a higher extent since mitochondria lack protection by chromatin structure and histones[51]. However, it is becoming increasingly evident that mitochondria possess similar DNA repair pathways as the nucleus[52].

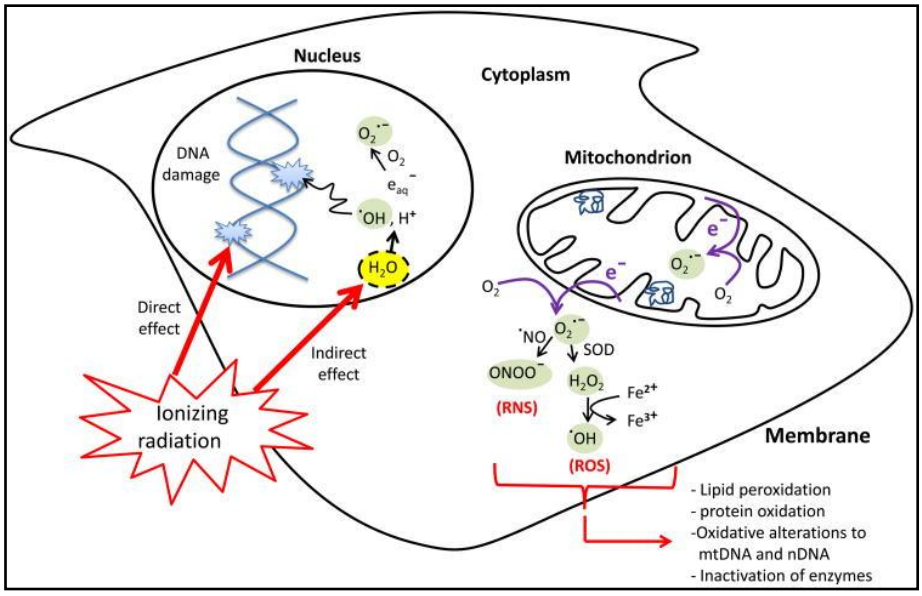

Figure 8. Direct and indirect cellular responses to ionizing radiation. Cellular damage by radiation can be caused directly by ionization of the biochemical structures or indirectly by generation of free radicals such as reactive oxygen (ROS) and nitrogen species (RNS) by oxidation processes, leading to consequences such as alterations in lipids, proteins, nuclear (nDNA) and mitochondrial (mtDNA) DNA. Adopted from [53].

The maintenance of DNA stability and integrity is essential to life, wherefore cells have developed several pathways to detect and efficiently repair DNA lesions caused by ionizing radiation[54]. Two major cellular DSB repair pathways known in the eukaryotic system are homologous recombination (HR) and non-homologous end-joining (NHEJ)[55]. Additionally to the repair mechanisms, cell cycle checkpoints exist (**Figure 9A**) which delay cell cycle progression, allowing more time for DNA repair. The final result of these pathways is cell cycle arrest by checkpoint activation and promoted DNA repair, or if the cell damage was too extensive, cell death is initiated, typically by apoptosis[56] (**Figure 9B, C**).

The mammalian cell cycle contains G0, G1, S, G2 and M phases (**Figure 9A**). Cells that are in the late G2 and the M phase, when their chromatin is decondensated in order to facilitate transcription and DNA replication, are the most sensitive to radiation[56]. The HR-mechanism can be regarded as an error-free pathway that utilizes a homologous template to replicate lost genetic material. Therefore, it is only active in proliferative cells during the middle and late S-phase and the G2/M checkpoint[49]. NHEJ allows the direct reconnection of broken DNA termini in non-cycling cells by excision of damaged nucleotides while operating without a template, making it more error-prone than HR[55]. NHEJ is thought to be mainly active during G1/G0 phases of cell cycle, when no sister chromatid is available in the cell to serve as a template for repair[49].

The recruitment and cooperation of many different proteins is required for each of the DNA damage response pathways. These proteins can be categorized into three groups including sensors, transducers and effectors (**Figure 9B**). The sensors, such as the Mre11/Rad50/NBS1-complex and the ATM kinase, scan the chromatin for damages and send a biochemical signal to modulate the function of other proteins. Downstream of the sensors, transducers like MDM2, p53, SIR1, CHEK2 or BRCA1, regulate signal transmission.

Finally, the effectors that include BAX, p21, CDK2, RAD51 and RAD50/MRE11 cause cell cycle arrest and DNA repair or apoptosis (**Figure 9B**)[56].

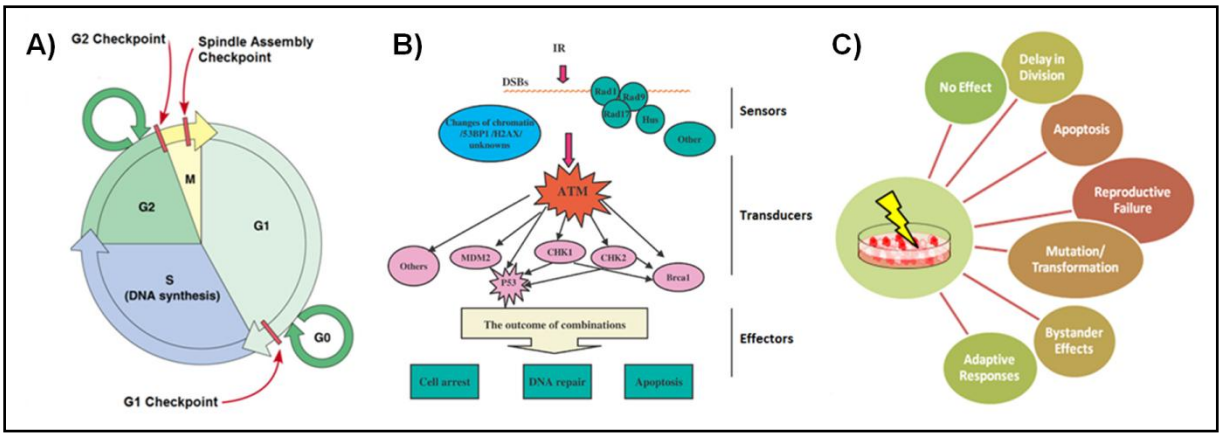

Figure 9. Cell cycle checkpoints, signal transduction cascade and outcomes of ionizing radiation. (**A**) A schematic representation of the different phases of the eukaryotic cell cycle is given. G0 indicates the quiescent phase where non-proliferative or differentiated cells rest. The G1 phase, where cell growth happens, finishes with the G1 checkpoint during which nutrients, cell size, growth factors and the DNA condition are checked. The subsequent S-phase where the DNA is duplicated is followed by G2-phase that prepares the cell for division. The G2-checkpoint ensures that the cell size and the duplicated DNA are fine. During M-phase, mitosis happens, and the intra-M checkpoint makes sure the chromosomes are attached to the spindle and the cells ready to be separated. (**B**) Sensor proteins recognize DNA damage, the damage signal is passed on to transducers that are downstream of the sensors, and the signal is passed on to the effector-proteins that finally are responsible for the different cell fates. (**C**) The different possible outcomes following ionizing radiation are summarized in this graphic. Adopted from [57-59].

p53, a crucial tumor suppressor protein that suppresses cancer, is one of the main transducer molecules that is activated in response to the various genotoxic stresses caused by ionizing radiation. It primarily acts as a sequence-specific transcriptional activator, and that for a wide variety of protein-coding and non-coding target genes[60, 61]. p53 works in the form of homo-tetramers that recognizes p53-responsive elements, activating or suppressing different promoters dependent on the situation of the cell[62].

Cellular stresses, such as DSBs, can result in ATM/ATR and Chk1/2 dependent activation of p53 that in response triggers processes such as apoptosis or senescence that limits the propagation of irreversibly damaged or malignant cells. In case of reparable damages, pro-survival signals are released that lead to programs such as temporary cell cycle arrest, DNA repair and anti-oxidant protein production[62-64].

p53 not only is the guardian of the genome, but also is involved in various other biological processes next to cell death, cell cycle arrest, senescense and DNA-repair, such as metabolism, autophagy, differentiation and development. The tumor suppressor p53, which is inactivated in most cancers, plays a critical role in the suppression of carcinogenesis. Mutations in one of the p53-allels already predispose humans to cancer quite early in life[4, 62].

Due to its biological importance, the expression of p53 is usually strictly regulated at different transcriptional and translational levels. A major regulator of the protein e.g. is MDM2 that under non-stressed conditions binds to and blocks p53's DNA binding, transcriptionally

activating domain. MDM2 also ubiquitinates p53, marking it for degradation by proteasomes[64, 65]. Upon encountering cellular stresses, p53 is stabilized via different mechanisms such as phosphorylation and deubiquitination, which then allows p53 to respond to the damage caused[64].

Involvement of p53 as a mediator for apoptosis is one of the main reasons for the gradual neural degeneration and death of neuron populations in neurodegenerative diseases, such as Parkinson disease or Alzheimer disease, which reflects p53's importance for the proper functioning of the nervous system. There are many studies on neurodegenerative diseases that suggest that p53 is a central player in neuropathogenesis[66-68].

Cell death and survival, proliferation and differentiation have to be delicately and dynamically fine-tuned during the development of the nervous system, for which different pathways are required that respond adequately to the specific cellular events. p53, being an inevitable member of these pathways, plays a crucial role as a decision-maker during neuronal development. Studies in mice show that one of the highest p53-expression levels during embryonic development is reached during the differentiation of neuronal precursor cells[69]. p53 not only plays a substantial role in neuronal apoptosis, but also in processes such as proliferation and differentiation of neural progenitor cells, axon guidance and axonal outgrowth and regeneration[69, 70].

The importance of p53 for normal neural development is further shown by studies in p53-null animals, where a significant amount of the animals die or develop exencephaly. The compensatory role played by p53's other two family members, p63 and p73, is the reason for the observed survival of a major amount of p53-null animals that bear a deletion of such a crucial gene[69]. Despite profound studies and already established widescale spectrum of p53-involved functions, newer involvements emerge with recent studies. The exact mechanism how p53 operates is still not entirely understood, but its involvement in the different cell fates following irradiation has been shown in different studies[71-74].

1.3.3. Prenatal exposure to ionizing radiation and the developing brain

It is generally assumed that proliferative cells are more sensitive to radiation compared to differentiated cells. Therefore, animals and humans are most vulnerable to radiation effects during the embryonic and early fetal periods of development[75]. Effects of prenatal irradiation include gross structural malformations, growth retardation, embryonic lethality, sterility and central nervous system abnormalities such as mental retardation and microcephaly[76]. Epidemiological studies, mainly carried out on atomic bomb survivors, report that there is a dose-dependent higher occurrence of severe mental retardation in children after *in utero* exposure to ionizing radiation, particularly when the exposure occurred during early gestational phases (weeks 8 to 15)[77] (**Figure 10**), a period which is characterized by rapidly proliferating and differentiating cells in the brain[30].

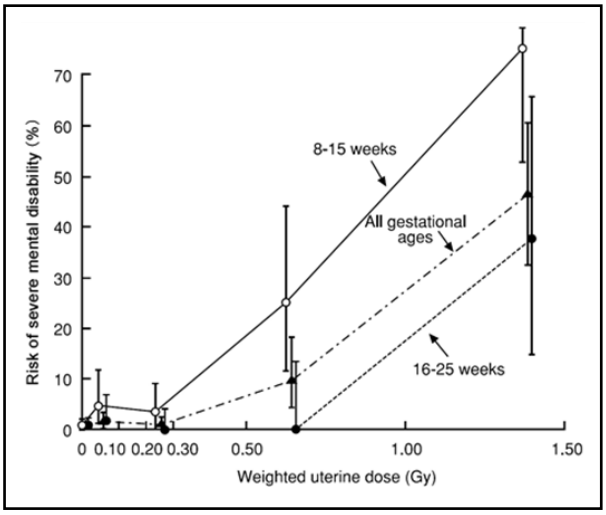

Figure 10. Mental retardation in prenatally exposed survivors of the atomic bombings of Hiroshima and Nagasaki. Significantly higher, dose-dependent occurrence of severe mental retardation was observed in children prenatally exposed to radiation (especially in those exposed in weeks 8-15 of pregnancy and, to a lesser extent in those exposed in weeks 16-25). Adopted from [77].

Supporting the results from human epidemiological studies, several animal studies have demonstrated the harmful consequences of prenatal exposure to ionizing radiation. In primates, fetal radiation exposure results in adult-onset of cognitive impairment[78, 79]. Various studies in mice and rats have revealed that pre-natal exposure to ionizing radiation leads to disruption of proper brain development, leading to the loss of neurons and reduced brain weight and size that result in behavioral differences[27, 80-82, 118]. In all cases the results were dependent on the radiation dose and the developmental stage at which the exposure occurred.

As previously mentioned, not all cells have the same radio-sensitivity. Cells that have a high division rate are more sensitive to radiation than those that are already specialized, since the DNA is most vulnerable during replication when the DNA is decondensed from the chromatin structure[83]. This is reflected in the so-called law of Bergonie and Tribondeau, who stated already in 1906 that the radiosensitivity of a cell is directly proportional to its proliferative activity and inversely proportional to the degree of cellular differentiation[84]. Despite some regions in the mature brain, such as in the caudate nucleus and hippocampus, where neurogenesis happens, the adult brain as a highly differentiated organ with low mitotic activity is considered relatively radio-resistant – completely in contrast to the developing brain[85].

1.4. The mouse as a model organism for understanding human brain functions

Mammalians can be divided into two groups based on their cerebral cortical folding: lissencephalic and gyrencephalic species. The gyrencephalic species like most primates and humans exhibit convolutions in the cortex, enabling bigger brain sizes and expanded surface area. The size and extent of folding of the cerebral cortex are the important factors that are

very distinct and vary between species and influence the species' intellectual abilities[17]. The mouse brain is smooth and about 2700 times smaller than the human brain in mass[86], which limits its ability to model more complex gyrencephalic brain structures. Even so, mouse model organisms are very popular for studies of neurological processes, brain development and neurological disorders[87].

The general structure of the brain is very similar between mammalian species. In contrast to the simple three-layered structure of the cerebrum of amphibians and reptiles, the surface of the mammalian neocortex is a more complex six-layered one[88], as previously mentioned. Apart from the neocortex, the hippocampus and amygdala are examples of extensively developed structures in mammals[89] that are evolutionarily conserved from mouse to man[86].

The rodent brain exhibits many of the key features of the human brain, including the general organization of the brain, the six-layered organization of the neocortex (**Figure 3C, D; Figure 11**) and the regionalization into sensory, motor and association areas[87]. Despite of the non-negligible difference in time scaling of brain development between human and mouse (**Figure 3A**), the sequence of key events in brain maturation, such as neurogenesis, neuronal migration, synaptogenesis, gliogenesis, oligodendrocyte maturation and age-dependent behaviors, are largely consistent between the two[90].

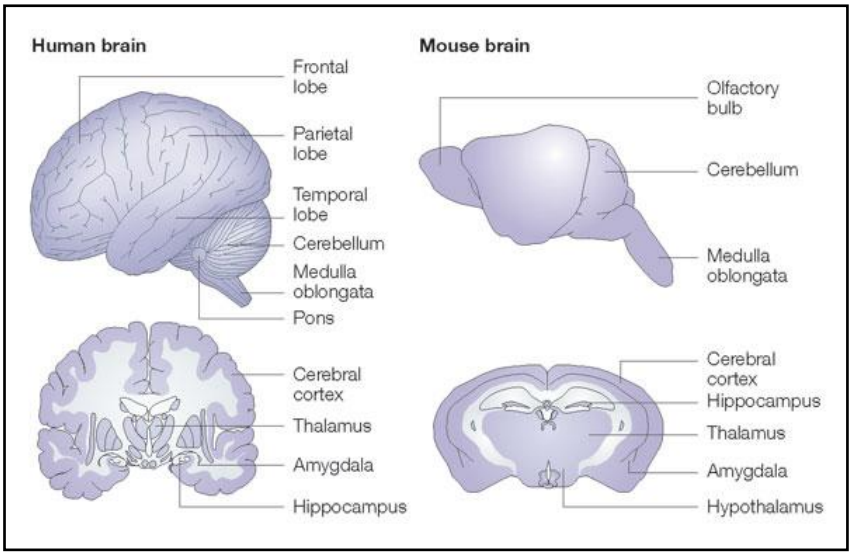

Figure 11. Comparison: General structure of the human and mouse brain. The greater size and convolutions of the cortex distinguish the human brain from the mouse brain. Nevertheless, both species possess many comparable structural features. Adopted from [86].

1.5. Early molecular effects of radiation on the developing mouse brain

It is the prenatal transcriptional processes that predominantly determine the anatomical and functional architecture of the brain[91]. During brain development billions of neural cells proliferate, are directed to differentiate and migrate to their specific locations where they mature and fulfill diverse functions. The engagement in their respective roles is accomplished by timely and regionally differentially regulated gene sets, which is why the transcription

profiles in developing brains are highly heterogeneous[92]. Today, we have various amounts of data from different research groups, who have attempted and partially succeeded in creating a complete map of the complex gene expression pattern during prenatal development, recording each change in gene expression at the many different coordinates in the brain, their timely and spatial dynamics[91].

To date, complete resolution has not been achieved concerning the question what causes the radiation-induced defects in embryonic brain development. In a recent study in mice, a set of early radiation-responsive genes could be identified. Among those genes, they found several genes of which only certain isoforms were differentially up-regulated after exposure to ionizing irradiation. These splice variants that were up-regulated in mice after irradiation were also highly enriched and up-regulated during brain development and *in vitro* neuronal maturation, suggesting involvement of these genes in important brain-related functions. Although many of the radiation-responsive genes were well known transcriptional targets of p53, involved in classical p53-mediated pathways like cell cycle arrest, DNA repair and apoptosis, a substantial number of the newly identified p53 targets had not been characterized until now[4].

Interestingly, a very strong overlap was observed between the gene expression profiles and phenotypes of the irradiated mice and several microcephaly mouse models[93, 94], suggesting that the early changes in gene expression during brain development might be the cause of late effects of radiation exposure such as microcephaly. It was therefore hypothesized that this alteration in expression can be associated with impaired cognitive functions after irradiation[4].

1.5.1. Radiation-responsive genes and the link to circRNAs

A remarkable and for us pivotal feature of the radiation-responsive genes, most of which are p53's targets, was that they are up-regulated during brain development and also enriched in the brain. Strikingly, we noticed that the circRNAs, a quite recently discovered RNA-species, show the same characteristic as the radiation-responsive genes: extra-ordinary enrichment in the brain and dynamic expression during brain development[1, 4]. Further investigation using the public data base "circbase.org" (developed by the Rajewsky lab at the Berlin Institute for Medical Systems Biology), showed that many of the radiation-responsive genes, such as *Pvt1* and *Ano3*, that have differentially expressed transcript variants, are also predicted to have circular isoforms. Interestingly, also adding to our interest in circRNAs, we found that most of the circRNAs are also evolutionarily conserved between mice and humans[1].

1.5.1.1. The radiation-responsive gene, *Pvt1*

The human *PVT1* gene is a long intergenic, noncoding RNA that resides in chromosome 8 and has oncogenic potential being a top target for alterations in various types of cancers, including breast and ovarian cancer, acute myeloid leukemia and Hodgkin lymphoma. *PVT1*

is homologous to the mouse plasmacytoma variant translocation gene *Pvt1* from chromosome 15. In both species, *PVT1* is located in a well-known cancer risk locus and has the popular oncogene *MYC* as its direct neighbor. *PVT1* is said to compete with endogenous RNA activity and to regulate protein stability of important oncogenes, especially of its neighbor *MYC*[95]. It has been shown to have several linear transcript variants[95] and is part of the radiation-responsive gene signature[4]. Computational analysis has suggested that linear *PVT1* transcripts strongly interact with the mir-200 family, acting as a sponge to these micro RNAs, thereby possibly regulating the expression of hundreds of mRNAs[95].

1.5.1.2. The radiation-responsive gene, *Ano3*

ANO3 encodes for a protein called anoctamin3 and is located on chromosome 11. It belongs to a family of closely related genes in sequence and topology, *ANO1-10*, that encode ion channels, such as calcium-activated chloride channels[96]. *ANO3* is differentially expressed in the central and peripheral nervous system, and has a close homolog in the mouse[97]. Molecular functions of *ANO3* are still poorly understood and controversial, but it is suggested that *Ano3* acts as a regulator of Slack, a natrium-activated potassium channel[97]. Mutations in anoctamin genes are responsible for various sets of diseases. *ANO3* has been shown to be involved in craniocervical dystonia[98], Alzheimer disease[99] and pain processing[100].

1.6. Circular RNAs (circRNAs)

miRNA, lncRNAs, snoRNAs or siRNAs are only few examples exhibiting the diversity of non-coding RNA molecules that have been discovered in recent years, additionally to the classic mRNAs, tRNAs and rRNAs[7]. Amongst them, circular RNAs (circRNAs) have been relishing more attention lately, ever since thousands of new circRNAs have been identified in eukaryotic cells thanks to present day's advanced deep sequencing technologies and computational techniques[107].

Different types of RNA circles have been classified until now, among which the exonic circRNAs make up the majority of the circRNAs identified in mammalian cells. These are a group of endogenous non-coding circular RNAs, mostly located in the cytosol[7] that can range in size between a few hundred to thousands of nucleotides in length. In contrast to the linear isoforms, circRNAs are formed by backsplicing events, where the 5' end of an upstream exon is covalently joined with the 3' end of a downstream exon that results in a closed loop structure[102] (**Figure 12**). Only very recently it was revealed that there exist mammalian circRNAs that consist of both exonic and also intronic sequences[103]. There is a large variety of genes, of different sizes and of different expression levels that can be flanked by different sized introns which can be backspliced to form circular transcripts[102, 103]. In this study, we focus on mammalian circRNAs that are formed via backsplicing of exonic and/or intronic sequences.

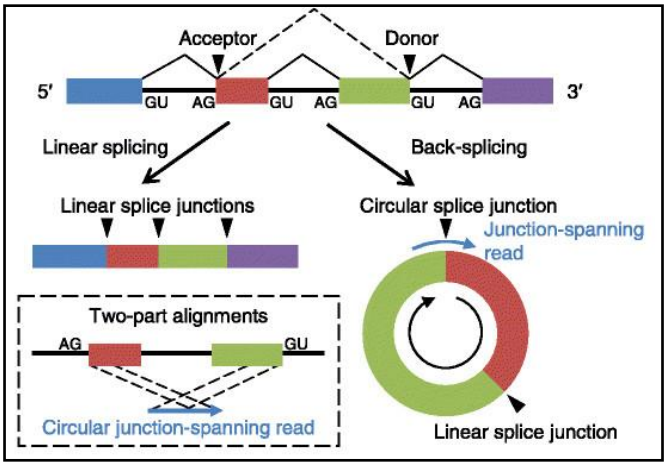

Figure 12. Backsplicing vs. normal splicing. Alternative splicing products of regular and back-splicing events are illustrated here. Exons are shown as colored boxes, introns as thin black lines in-between. The linear splice junctions are shown as angled continuous black lines; the circular junctions are marked by the angled broken black lines connecting exons. The junction spanning reads in the circular splice junction that are identified by the computational programs are indicated in light blue. Adopted from [101].

1.6.1. circRNA biogenesis

Although not entirely explored yet, there exist different models that describe possible mechanisms how the backsplicing sites are brought to close proximity promoting circularization. One hypothesis suggests that intron lariats that are created by skipping alternative exons can bring non-linear splicesites together, facilitating circularization. Other evidence suggests that base-pairing of flanking inverted repeats or ALU elements might bring the backsplice sites together leading to circularization (**Figure 13A**). Yet another possibility is that RNA binding proteins that actively build bridges between the backsplice sites are involved in the biogenesis of circRNAs[7, 104].

1.6.2. Importance of experimental validation of the predicted circRNAs

Thousands of new circRNAs have been recently added to the databases, largely based on computational analysis of RNA-sequencing data that rely on circular junction spanning reads[1], which unfortunately also includes spurious evidence of circRNAs. The scrambled exon-exon junctions that the algorithms screen for, where the ordering of the exons in a sequence is reversed relative to the annotated linear transcripts of the source gene, can also be a result of reverse transcriptase template switching, DNA rearrangements and tandem duplications or trans-splicing events (**Figure 13B**), that only appears as a circular junction[105].

An occurrence of such an event can be experimentally determined by using divergent primers for qRT-PCR that are oriented to amplify away from each other, only resulting in amplified products when exon-shuffeling has occurred resulting in scrambled junctions that brings together outside sequences, turning the primers convergent. In order to exclude the

only apparent backsplice-junctions, it is necessary to additionally verify that these findings really are circular RNAs. Safe validation of the circularity of the predicted circRNAs can be achieved using different methods[105].

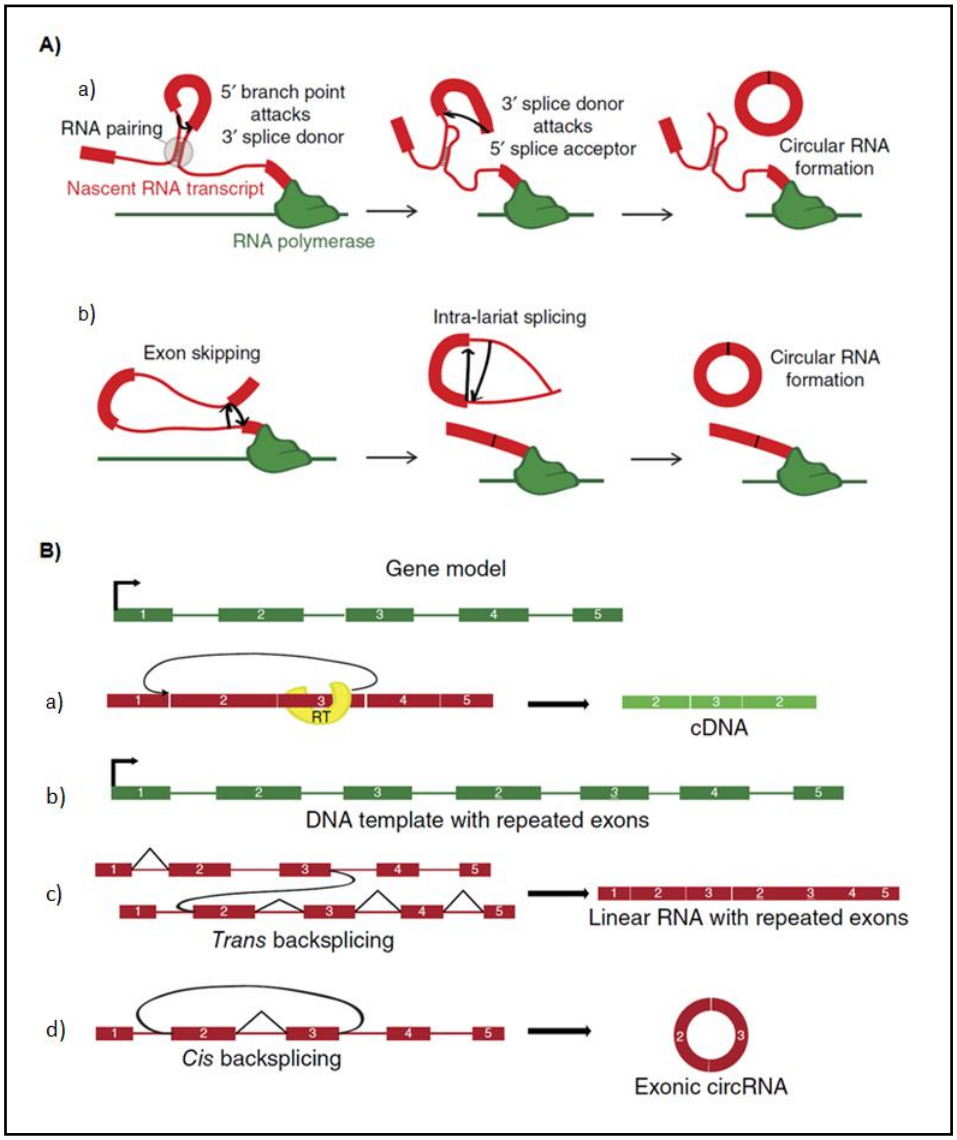

Figure 13. circRNAs biogenesis and alternative mechanisms leading to scrambled exon-exon junctions. (**A**) Two proposed mechanisms are illustrated here that could promote backsplicing. Base-pairing of flanking inverted repeats (**a**) could be responsible for bringing the splice sites together, promoting circularization. Intron lariats that are created by skipping alternative exons could bring the splicesites into close proximity (**b**), again promoting circularization. (**B**) The alternative mechanisms that could result in apparent circular junctions are illustrated here: Reverse transcriptase template switching (**a**), tandem duplications (**b**), transbacksplicing (**c**) and backsplicing (**d**). RT: Reverse transcriptase. Adopted from [105].

An important common feature of circRNAs is that they do not have any 3' or 5' ends that can be attacked and degraded by exonucleases. Hence, the circRNAs are resistant to exonucleases and often more stable than linear RNAs[7] (**Figure 14A**). Also, while linear exonic RNAs usually have 3' polyadenylations, the circular RNAs lack these. Both these characteristics can be used for the validation of circRNAs. Treatment of total RNA samples with the exonuclease RNaseR that degrades only linear species prior to a qRT-PCR, or by

comparison of cDNA synthesis using either random hexamer primers or oligo-dT primers before qRT-PCR (**Figure 14B**), the latter of which are not able to reverse transcribe circRNAs because these lack the poly-A tail, finally enables safe verification whether the expression that is observed with the divergent primers really comes from backsplicing events, or only apparent ones[7, 105].

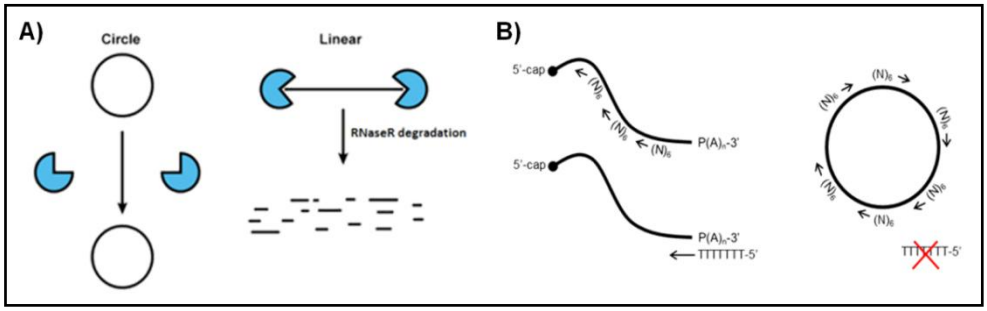

Figure 14. RNaseR treatment and the usage of oligo-dT vs. random hexamer primers. (**A**) The circular transcripts are resistant to the exonuclease RNaseR, while the linear transcripts are degraded. (**B**) Random hexamer primers can bind randomly on the linear as well as on the circular transcripts, delivering cDNA during reverse transcription; the oligo-dT primers can only bind on the polyA-tails of the linear transcripts. Adapted from [7, 106].

1.6.3. Functions of the circRNAs

The one most prominent and clearly proven function of the circRNAs is their activity as miRNA-binding sponges. Recently, it was shown that circRNAs can contain multiple copies of miRNA binding sites within them that can target miRNAs. By binding the miRNAs, circRNAs hinder the miRNAs in their original function: RNA silencing and post-transcriptional regulation of gene expression (**Figure 15A**). This has to date been successfully demonstrated for two circRNAs, circCDR1as and circSry[2, 3].

An involvement of the circRNAs has also been shown in the regulation of alternative splicing, mRNA expression, transportation of various factors and sponging of other factors such as RNA binding proteins (**Figure 15B, C, D, E, F**)[109].

There exist several circRNAs that contain start codons and reasonable open reading frames, but neither an association with ribosomes or an internal ribosome entry site in circRNAs has been observed until now, which is why, to date, the circRNAs are assumed not to be translated (**Figure 15G**)[7, 110]. The functions of the large majority of circRNAs are still scarcely understood and require more directed investigation.

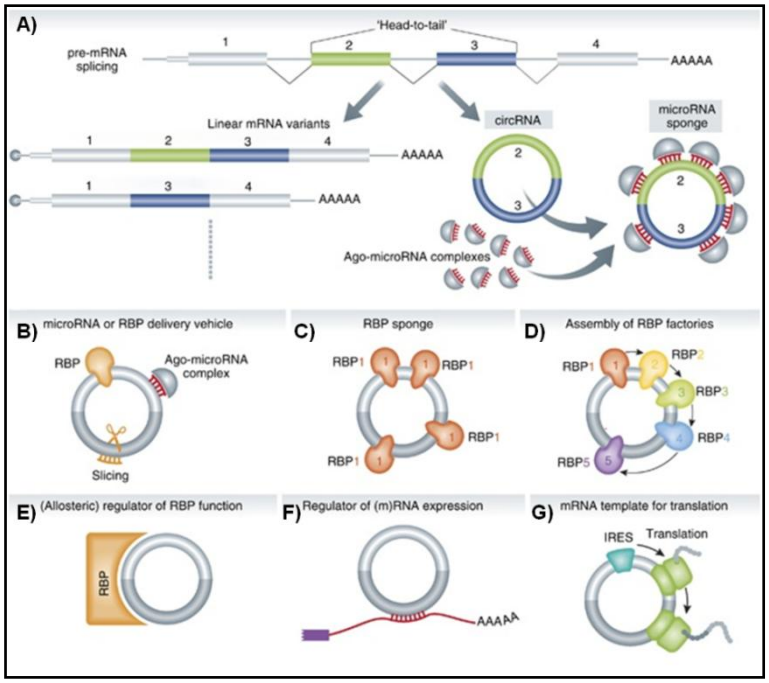

Figure 15. circRNAs' functions. (**A**) The most important and already proven function of the circRNA is its activity as miRNA targeting sponge. (**B**) An involvement of circRNAs as transportation vehicle of different proteins or miRNAs and (**C**) as sponges for RBP has also been proposed. (**D**) circRNAs may also play a role as an assembling factor of RBP factories, (**E**) as a regulator of RBP and (**F**) mRNA expression. (**G**) Associations with IRES have not been found yet, but hypotheses exist that some may also code for proteins. RBP: RNA binding protein; IRES: Internal ribosome entry site. Adopted from [111].

2. Objectives of this study

Looking at previous research results and data from the public data base circBase.org, we had learned that many of the radiation-responsive genes are predicted to have circular transcript variants. So, our very first aim was to validate whether these predictions are true, whether we really have circular transcripts' expression. In this study, we mainly concentrated on the expression of the radiation-responsive genes *Pvt1* and *Ano3*, which are genes that were predicted to have circular isoforms.

Having the mouse at disposal as a perfect model organism for neuro-developmental studies, we decided to perform *in vivo* and *in vitro* gene expression studies of the mouse at different developmental stages, mainly using neuronal cells.

One of the first things we planned to investigate on, in case we were to successfully validate the circRNAs, was the circRNAs' stability; based on theoretical information, we had assumed the circRNAs to be more stable than their linear counterparts. Knowing that circRNAs are generally said to be induced during brain development and enriched in the brain, we were interested in our circRNAs' expression during brain development and neuronal maturation. Also, we were ambitious to investigate into circRNAs' tissue specificity.

Having radiation-responsive source genes and not any published insights about circRNAs' responsiveness to radiation, we were also eager to know whether the circRNAs' expression is influenced by exposure to radiation. We were curious to know whether these circular transcripts can be included to the radiation-responsive gene signature.

One of the things about circRNAs, where we only have scarce knowledge till now, is about its functional involvement in the cell. Its abundance and evolutionary conservancy suggest that many more functions are to be found for the newly rediscovered RNA species than the already known ones. Gaining more insights to circRNAs' functions was also one of the targets of this study.

3. Materials and Methods

3.1. Animals and primary neuron cell cultures

All animal experiments were carried out in accordance with the European Communities Council Directive of November 24, 1986 (86/609/EEC) and were approved by the local SCK·CEN/VITO ethical committees (ref. 02- 012). Wild-type C57BL/6J mice were purchased from The Jackson Laboratory and housed in a specific pathogen-free animal facility at SCK·CEN. The animals were held under controlled conditions, and a standard 12:00/12:00 light/dark cycle was maintained. Food and water were available *ad libitum*. In order to ensure synchronous timing of embryonic development the differences in times of fertilization was minimized. Therefore, mice were coupled only during a short period between 08:00 and 10:00 in the morning, and the day of fertilization is referred to as day 0 (E0).

Pregnant mice whose embryos are at either embryonic day 11 (E11), 12 (E12), 15 (E15) or 18 (E18) were sacrificed by cervical dislocation, the embryos isolated and decapitated. Then, either whole embryonic brains (E11, E12, E18) were taken for RNA extractions and subsequent qRT-PCRs for *in vivo* experiments, or cortices and hippocampi (E15) were separated by micro-dissection and primary neuron cell cultures were prepared for *in vitro* experiments. The cell cultures were prepared according to the protocol described in Samari et al., 2013[112].

Also, post natal mice at the ages post natal day 10 (P10), 30 (P30) and adult (Ad) were sacrificed for the respective experiments, their organs (mostly brain) isolated and taken for RNA extractions.

3.2. Ribonuclease R (RNaseR) treatment

RNA purified from mouse brain at P10 was taken to treat with 1, 3 and 10 U of RNase R/µg of total RNA. A non-treated sample served as control. RNaseR treatment was performed in a reaction mix that included RNA (2 µg of total RNA), RNaseR (Epicentre RNR07250), 10xRNaseR Buffer that is provided by the company together with the enzyme and respective amount of water to achieve a total reaction volume of 25 µl. This mixture was then incubated at 37°C for 15min. Subsequently the volume was adjusted to 100 µl using RNase-free water.

For further processing the Qiagen AllPrep DNA/RNA Mini Kit was used. After adding 350 µl of RLT buffer, the samples were homogenized well before proceeding with the addition of 250 µl of 96-100% EtOH. The samples were then transferred to the RNA-binding columns, centrifuged for 15 seconds at > 8000 x g and the flow-through was discarded. The column was then washed with 500 µl of RPE buffer, and subsequently with 500 µl of 80% EtOH. Finally, making sure the column is free of EtOH, RNA was eluted with 30 µl of RNase-free water by centrifugation for 2 min at > 8000 x g.

3.3. Actinomycin D treatment

Primary cortical neuronal cultures after seven days *in vitro* (DIV7) were treated with Actinomycin D (solubilized in DMSO) at a concentration of 1 µg/ml. RNA-extractions were performed 1, 2, 4, 8 and 24 h after treatment. Cultures that were treated with just DMSO served as timepoint zero/control.

3.4. Neuronal Maturation

For neuronal maturation experiments, primary cortical and hippocampal neurons were isolated from E15 embryos, differentiated in Neurobasal/B27 medium as previously described[112] and total RNA was extracted at DIV1, 3, 7, 10 and 14. Replacement of growth medium after 3 days was not done.

3.5. Brain Development

In order to analyze expression of circRNAs during brain development *in vivo*, total RNA was extracted from mouse brains at different embryonic and post-natal developmental stages: E12, E18, P10, P30 and adult mice.

3.6. Tissue specificity

For determining tissue specificity, several tissues (brain, eye, heart, kidney, liver, lung, spleen and white adipose tissue) were dissected from adult wild-type C57BL/6J mice for total RNA extraction.

3.7. X-irradiation: *in vivo* and *in vitro*

At E11, pregnant female mice used for *in vivo* studies were whole body irradiated with 1 Gy at a dose rate of 0.35 Gy/min using a Pantak RX, 250 kV-15 mA, 1 mm Cu filter installation. The calibration of this X-ray tube was done using an ionization chamber. Control-mice were sham-irradiated. Mice were sacrificed 2 h post irradiation, embryos separated and decapitated. The brains were then used for RNA extractions. For *in vitro* experiments, primary neuronal cultures from E15 mice brain were irradiated (1 Gy) 24 h after being in culture, using the same setup as for *in vivo* experiments; and RNA extraction was performed 6 h post irradiation. Sham-exposed cells subjected to the same conditions were considered controls.

3.8. Cell lysis and RNA extraction

Qiagen's AllPrep DNA/RNA Mini Kit was used to purify RNA from embryonic mouse tissue samples and neuron cells from culture. The extraction was carried out as described in the protocol provided by Qiagen, but using RLT-buffer supplemented with 1% β-Mercaptoethanol. At the end, 30 µl of RNase free water was used to elute the RNA from the columns and a micro-volume spectrometer (Xpose™ - Touch & Go) was used to determine the RNA concentrations in the elution.

3.9. Reverse Transcription – cDNA synthesis

The GoScript™ Reverse Transcription System by Promega was used according to provided instructions to prepare cDNA from the purified RNA. 1 µl of random hexamer primers and 3.75 mM $MgCl_2$ were taken for a 20 µl-reaction. First-strand cDNA was synthesized from 2 µg of total RNA, or in case the RNA concentration was low, the maximum amount possible was used in a 20 µl reaction.

For reverse transcriptions using oligo-dT primers, the random hexamers were substituted with1 µl of oligo-dT primers, but otherwise the protocol remained unmodified.

3.10. qRT-PCR

For qRT-PCR, the MESA GREEN kit from Eurogentec was used according to the manufacturer's instructions. Each reaction was performed in duplicates and consisted of a total volume of 25 µl that included 200 nM of forward and reverse primers, the MESA GREEN mastermix and the template cDNA synthesized as previously described. The 96-well format, high-speed thermal cycling 7500 Fast Real-Time PCR System by ThermoFisher was used to perform the reactions.

The programmed setting started with an initial step of 5 minutes at 95 °C to activate the enzymes, followed by 40 cycles of denaturation for 3 seconds at 95 °C and primer annealing and elongation for 45 seconds at 60°C. Subsequently, the melting curve program was run to check for additional PCR products and primer dimers. Reaction efficiencies were taken for relative quantification of RNA expression as described by Pfaffl, 2001[113]. *Gapdh* and/or *Polr2a* served as internal reference genes. Details to all primers used for the qRT-PCRs here are available upon request.

3.11. qRT-PCR using miRNA

Qiagen's miRNeasy Mini Kit was used to extract total RNA from cortical cells that include miRNA. cDNA synthesis was performed using the miScript II RT Kit by Qiagen with the miScript HiFlex Buffer. Both procedures were performed according to the protocols provided

by the company. E15 mouse brains were used to seed cortical neuron cultures and total RNA including miRNA was extracted on DIV1, 3 and 7. miScript Primer Assays and the miScript SYBR Green PCR Kit from Qiagen were used for subsequent qPCRs. The housekeeping gene *RNU6-2* was taken as a reference gene for miRNA expression.

4. Results

4.1. Validation of circularity of predicted circular transcripts of radiation-responsive genes *Pvt1* and *Ano3*

Several circular transcript variants were found to be predicted for the genes *Pvt1* (**Figure 16A**) and *Ano3* (**Figure 16B**) that were chosen for further investigation from the previously mentioned radiation-responsive gene signature. In order to verify the expression of these predicted circRNA isoforms, outward-directed, or divergent primer-sets were designed for each candidate, spanning the probable circular backsplice sites (**Figure 16A, B**). These primers were expected not to deliver any products when only the linear transcripts are present during a polymerase chain reaction (PCR). Presence of the circular transcripts though, where due to the circularization the originally divergently designed primers would end up facing each other again (**Figure 16C**), was expected to lead to PCR products. qRT-PCR was then performed on total RNA samples extracted from mouse brain tissues at different developmental stages. Out of five predicted circular isoforms for *Pvt1*, clear amplification was observed for three transcripts, while for *Ano3* four out of five predicted circular variants generated a product using the outward-facing primers (**Figure 16A, B**). The sizes of the PCR-products were determined by agarose gel electrophoreses (**Figure 16D**) that revealed amplicons in the expected sizes for each of the seven circular transcripts.

To further verify the circularity of the candidates, two additional steps were conducted. First, qRT-PCR was performed on exonuclease RNaseR digested total RNA samples extracted from mouse brain at P10. Expression of the circular transcripts (named “circ-XXXX” accordingly) of each gene was compared to their linear counterparts (“Pvt1_Ex 8-9” and “Ano3_Ex 3-4”, respectively). Additionally, *Gapdh* was used as a linear mRNA control. A total of 2 µg RNA was treated with 0 U, 2 U, 6 U and 20 U of RNaseR. The treatment resulted in a dose-dependent degradation of all linear mRNAs, while none of the circular RNAs were degraded. Not only did the circular transcripts show resistivity to RNaseR treatment, but an arguably increased amplification of the circRNAs could be observed with higher RNaseR concentrations (**Figure 17A, B**).

As a second method to verify the same, reverse transcription using oligo-dT primers and random hexamer primers was compared when doing the qRT-PCR. Both linear and circular transcripts, of *Pvt1* as well as of *Ano3*, were quite efficiently reverse-transcribed when using random hexamer primers for the cDNA synthesis. In complete contrast, usage of oligo-dT primers did not generate any cDNA for the circular *Pvt1* candidates, but only for the linear one. The linear *Gapdh*-control-RNA was also transcribed in a comparable manner as with random hexamers. Notably, the linear transcript of *Pvt1*, for which the designed qPCR-primers are located more towards the 3’-end, showed an even enhanced expression when oligo-dT primers were used that bind to polyadenylated 3’-ends. Similarly, cDNA synthesis was clearly not efficient when using oligo dT primers instead of random hexamers for the *Ano3*-circular transcripts, though a pre-eminent contrast to its linear transcript was not observed here (**Figure 17C, D**).

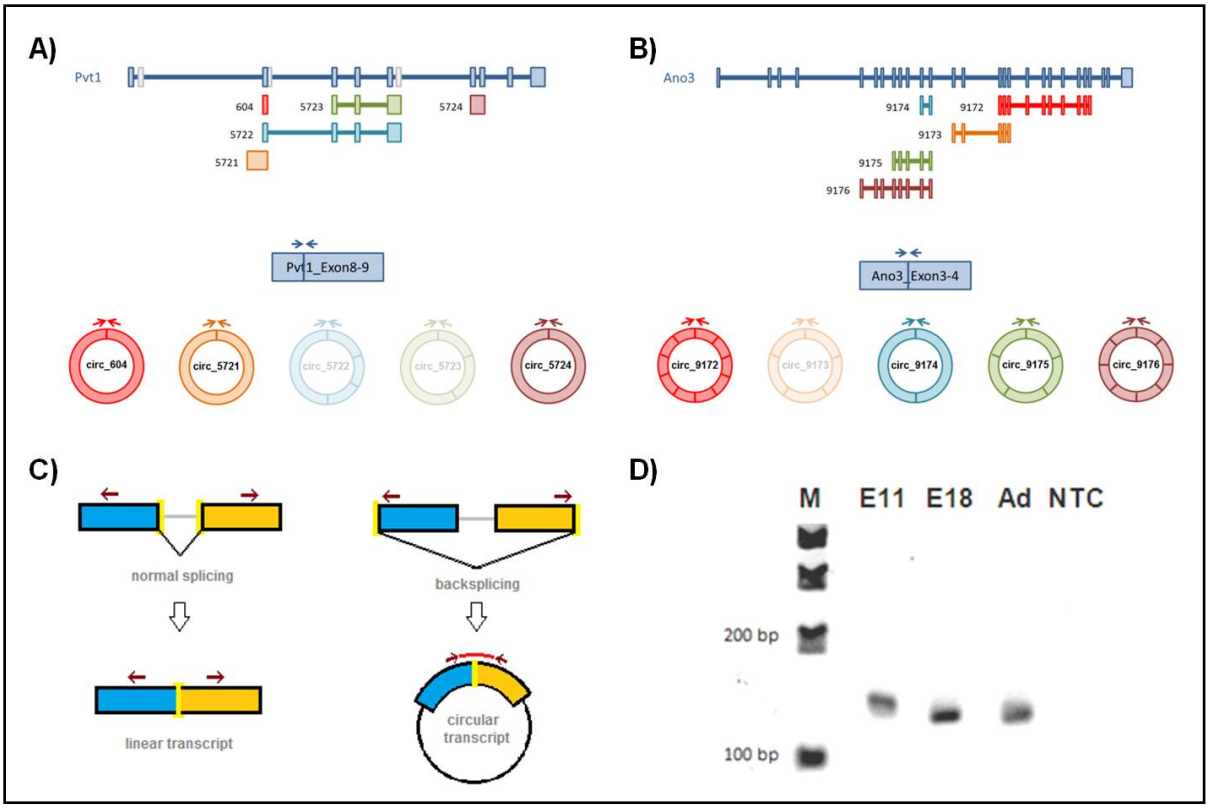

Figure 16. Amplification of circRNA using divergent primers. Genomic structures of the genes *Pvt1* (**A**) and *Ano3* (**B**); the exons are shown as boxes. Beneath, their predicted circular splice variants' origins are indicated, showing which exonic and intronic regions of the gene make up the respective predicted circRNA. Below that, the different circular transcript variants and their linear counterparts are depicted, with arrows indicating the divergent or convergent qRT-PCR primers that were designed in the circular or linear splice junctions, respectively. The faded representations of the circRNAs show the predicted circRNAs that were ruled out due to their nonexistent expression under the tested conditions. circ_XXXX: circular transcripts; Pvt1_Ex 8-9: linear transcript of *Pvt1*; Ano3_Ex 3-4: linear transcript of *Ano3*[106]. (**C**) The validation strategy of circRNA expression using divergent primers is represented in this illustration. Amplification can be achieved using divergent primers (marked by arrows) when circularization of the transcript (backsplicing) makes the outward-directed primers face each other[3]. (**D**) qRT-PCR using divergent primers generated PCR products of expected sizes. The gel-image shows the distinct appearance of the band at the expected size (here: 125 bp; shown is the result of gel electrophoresis for circ_5724). M: Size Marker; E11, E18: brain tissue from E11, E18; Ad: adult brain; NTC: non-template control.

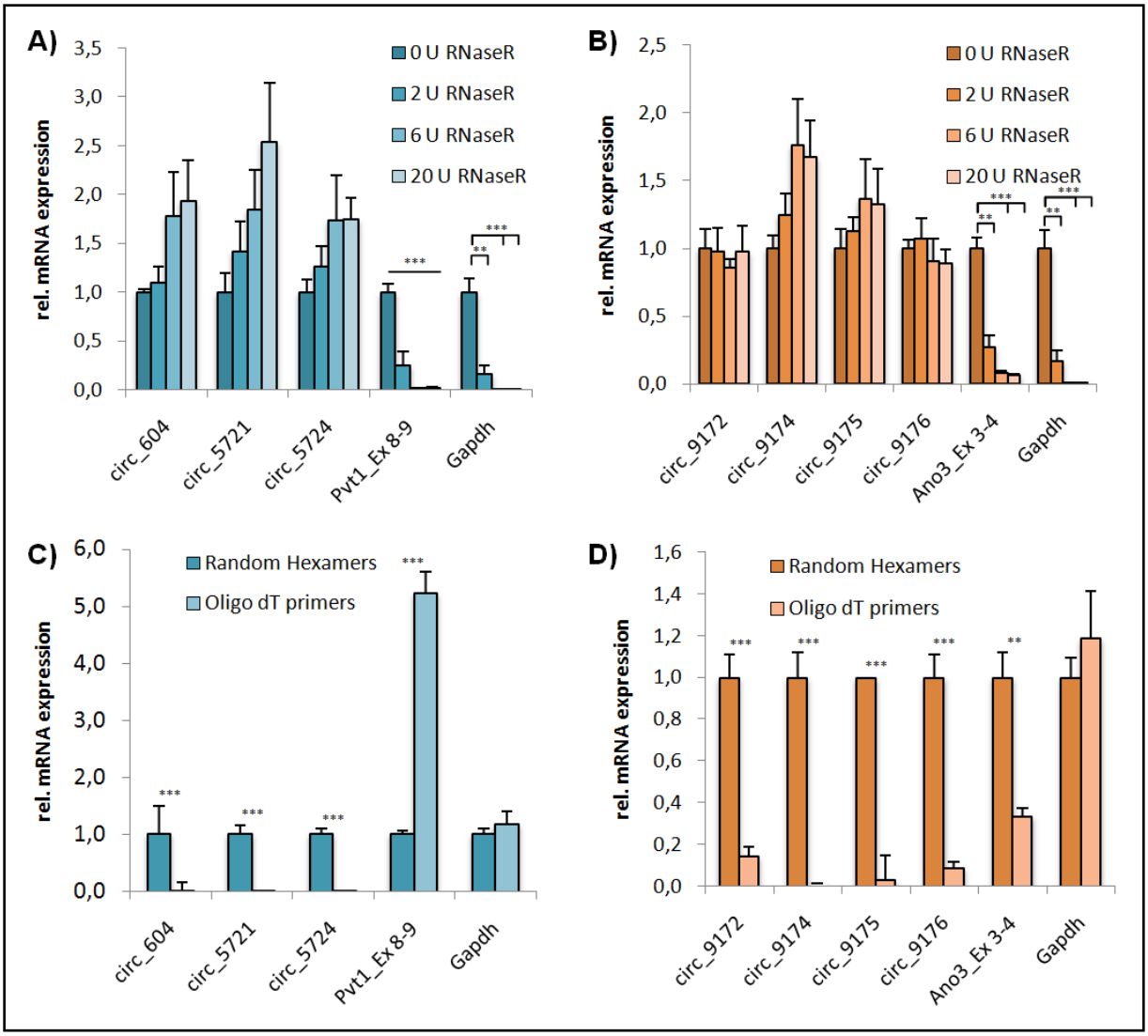

Figure 17. Experimental verification of circularization. Difference in expression of the transcript variants of *Pvt1* and *Ano3* was assessed via qRT-PCR using RNaseR treated RNA samples (**A, B**) and using random hexamer vs. oligo-dT primers for reverse transcription of qRT-PCR (**C, D**). Circular transcripts ("circ-XXXX") of *Pvt1* (**A, C**) and *Ano3* (**B, D**) are compared to their respective linear counterparts and the linear mRNA of *Gapdh*. Data shown are means of four replicates and have been normalized against 0 U RNaseR or random hexamers. The indicated error bars represent standard errors. *p<0.05; **p<0.01; ***p<0.001 (Student's t-test).

4.2. Radiation-responsive genes *Pvt1* and *Ano3* express stable circular transcripts

The Actinomycin D stability assay, an assay that uses an antibiotic agent leading to the inhibition of cellular transcription by intercalation to the DNA and blocking the progression of RNA polymerase, was performed to determine and compare the stability of circular and linear RNAs. RNA of primary cortical neurons at DIV7 was extracted after 0, 2, 4, 8 and 24 h of Actinomycin D treatment. TATA binding protein (*Tbp*) and *c-Myc* were used as controls for short half-life genes[104] and *Gapdh* was used as a control for stable mRNA (**Figure 18A**).

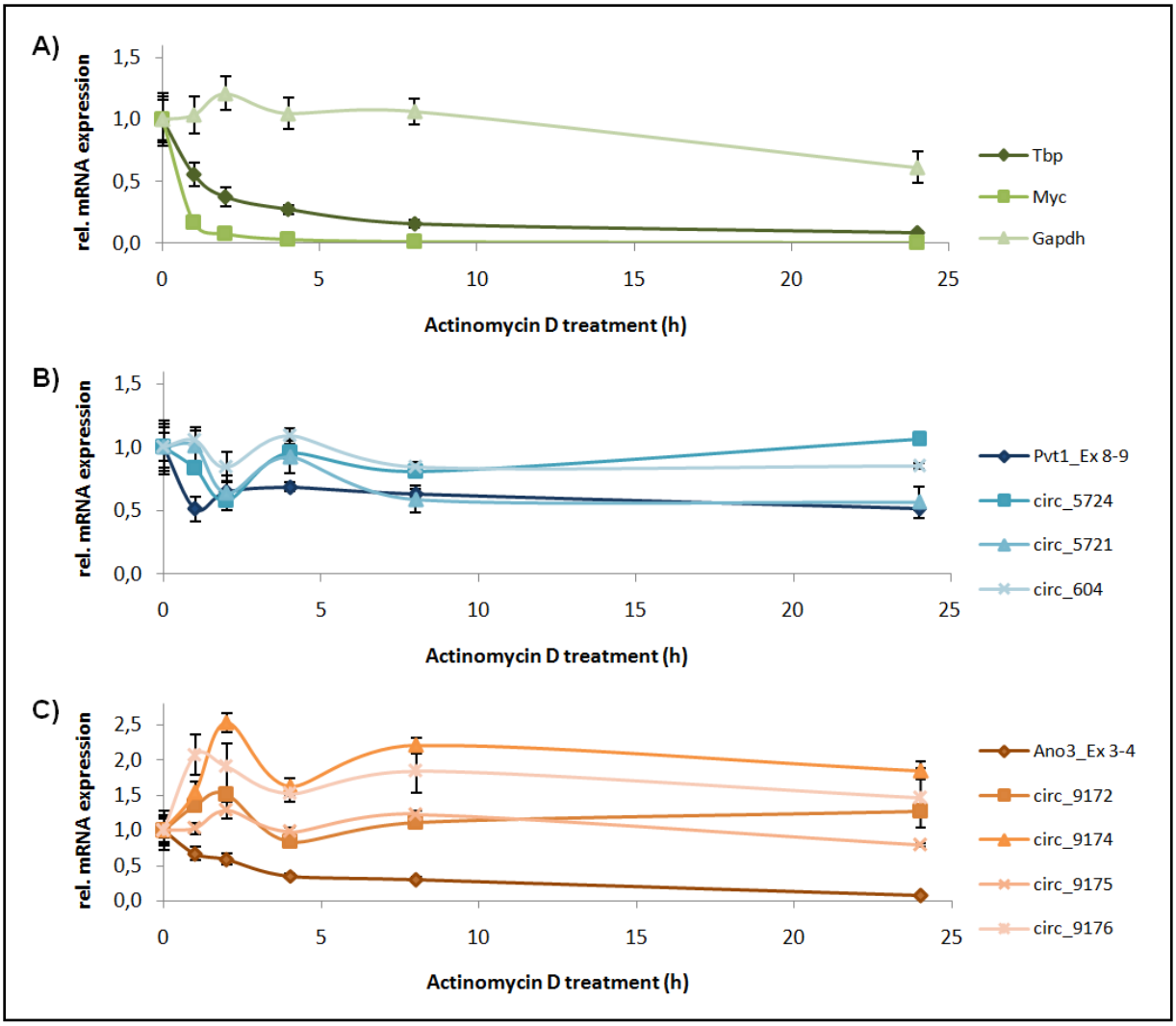

Figure 18. Stable *Pvt1* and *Ano3* transcripts after 24 h of Actinomycin D treatment. Relative expression levels corresponding to the stability of the genes at the different times points after treatment are given in the graphs above (**A**: reference genes *Tbp*, *Myc* and *Gapdh*; **B**: *Pvt1* transcript variants; **C**: *Ano3* transcript variants). Data shown are means of four replicates and the indicated error bars represent standard errors.

All *Pvt1* transcripts, as well as *Ano3* circular transcripts remained non-decayed and relatively stable after 24 h of Actinomycin D treatment, indicating long half-lives. The linear *Ano3*-transcript showed a decay pattern similar to that of the instable control gene *Tbp*, indicating lower stability than its circular transcript variants (**Figure 18B, C**).

4.3. *Pvt1*-circRNAs and *Ano3* transcripts are highly enriched in the brain

Our current relatively moderate knowledge about circRNAs claims enrichment of a large part of circRNAs in the mammalian brain[1]. This suggested the existence of a similar differential tissue specific expression pattern for our newly discovered circular transcripts. RNA samples from different tissues of adult mice, such as brain, eye, heart, kidney, liver, lung, spleen and white adipose tissue, were dissected to investigate the tissue distribution of *Pvt1* and *Ano3*

transcripts. Circular transcripts of *Pvt1* showed high enrichment in the brain, while the linear transcript was most expressed in the liver. In contrast, all *Ano3* variants, including the linear mRNA, were solely expressed in the brain and the eye (**Figure 19**).

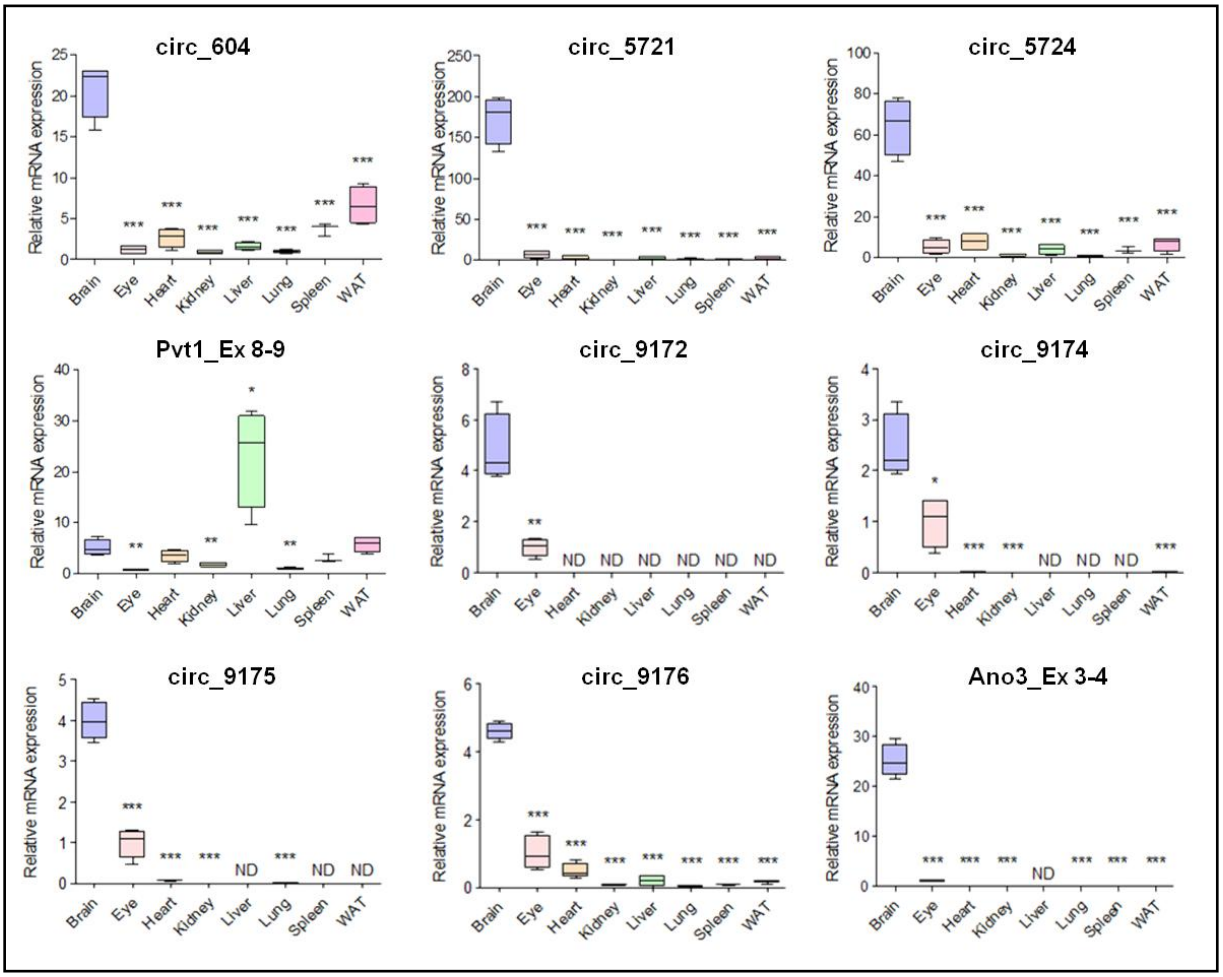

Figure 19. Tissue-specific expression of circular transcripts of *Pvt1* and *Ano3* in comparison to their respective linear counterparts. Expression levels for each *Pvt1* and *Ano3* transcripts are given as box plots for 8 different tissue types (*Pvt1*: relative to lung; *Ano3*: relative to eye; n=4). For comparisons between brain and other tissues a paired Student's t-test was used (*p<0.05; **p<0.01; ***p<0.001). WAT: white adipose tissue; ND: not detected.

4.4. Linear and circular transcripts of *Pvt1* and *Ano3* are induced during neuronal maturation in primary cortical and hippocampal neurons

From a previous publication, we already knew about the up-regulated expression of *Ano3*'s linear transcript during neuronal differentiation[4]. Additionally, knowing that the circRNAs are generally said to be induced in maturing and differentiating neurons[1], and having now shown the enrichment of our circular transcripts mostly in the brain, next we decided to investigate the expression of linear and circular *Pvt1* and *Ano3* transcripts during *in vitro* neuronal maturation of primary cortical neurons. RNA was extracted on DIV1, 3, 7, 10 and 14 for subsequent qRT-PCRs. In general, all *Pvt1* (except circ_5724) and *Ano3* (except circ_9176) transcripts are induced during maturation. For *Ano3*'s circular transcripts, this up-regulation is

mostly obvious after DIV10 only (**Figure 20B**), while *Pvt1*'s transcripts are induced a little earlier during maturation (**Figure 20A**). Interestingly, the expression of the linear *Pvt1* isoform peaked at DIV7 after which it gradually decreased, while the circular transcripts remained highly expressed at least until DIV14 (**Figure 20A**). *Ano3*'s linear transcript though seems up-regulated also after DIV7 (**Figure 20B**). Similar results were also achieved in primary hippocampal neurons for *Pvt1* (see Annex: **Figure I**).

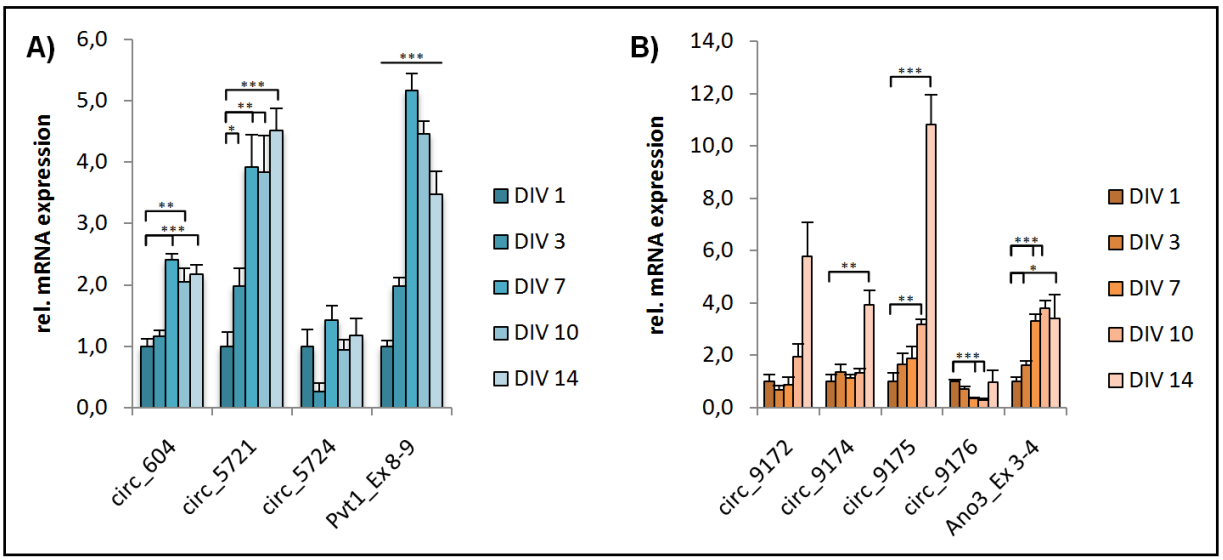

Figure 20. Induction of *Pvt1* and *Ano3* transcripts during neuronal maturation. Relative expression of linear and circular transcripts of *Pvt1* (**A**) and *Ano3* (**B**) is shown during cortical neuron maturation. Data shown are means of four replicates and the indicated error bars represent standard errors. DIV: days *in vitro.* *p<0.05; **p<0.01; ***p<0.001 (Student's t-test).

4.5. circRNA expression is enriched during *in vivo* brain development

In order to determine the expression of the different *Pvt1* and *Ano3* transcripts during *in vivo* brain development, qRT-PCR was performed using RNA extracted from brains of E12, E18, P10, P30 and adult mice. All circular *Pvt1* transcripts were gradually up-regulated with increasing age until adulthood, whilst the expression of the linear mRNA increased until P10 and declined thereafter (**Figure 21A**). For *Ano3*, all transcripts were induced and showed increased expression until adulthood, but that increment is evident only after P30. Also, the *Ano3* linear transcript as opposed to the linear one of *Pvt1* only shows increased expression after P30 and does not show any significant decline in expression thereafter (**Figure 21B**).

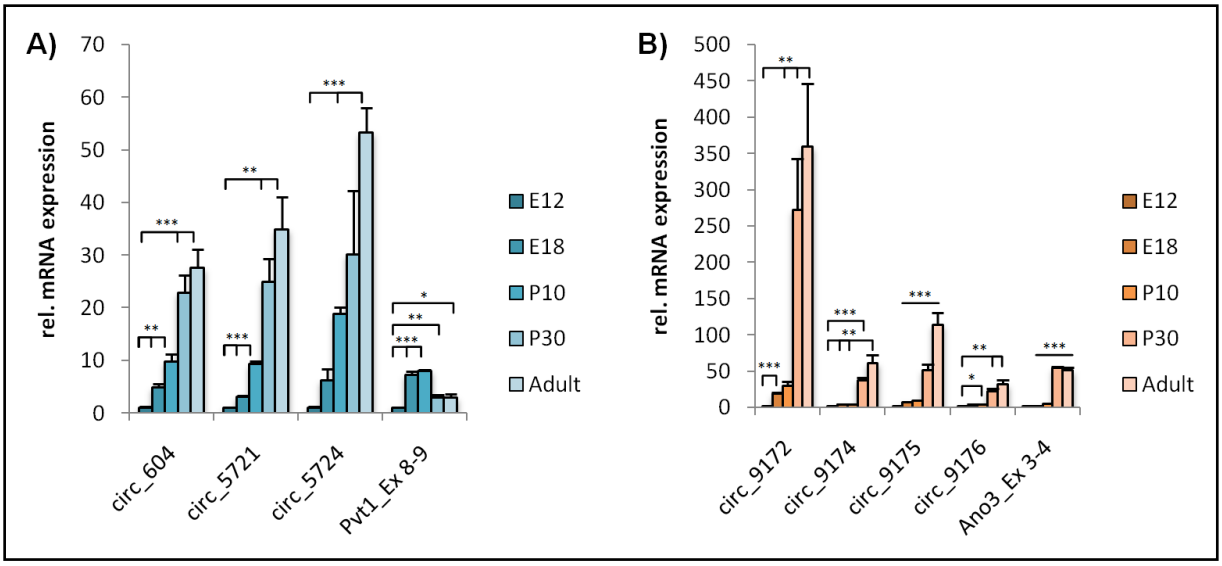

Figure 21. Expression of *Pvt1* and *Ano3* transcripts during *in vivo* brain development. Relative expression of *Pvt1* (**A**) and *Ano3* (**B**) transcripts are shown during different stages of brain development from embryonic to adult brain. Data shown are means of four replicates and the indicated error bars represent standard errors. E12, E18: embryonic day 12, 18; P10, P30: post natal day 10, 30. *p<0.05; **p<0.01; ***p<0.001 (Student's t-test).

4.6. Up-regulation of *Pvt1* and *Ano3* circular transcripts in primary cortical and hippocampal neurons after irradiation

Previously, the linear transcripts of *Pvt1* and *Ano3* had been shown to be highly induced after irradiation[4]. In order to determine the radiation-induced changes in expression of the *Pvt1* and *Ano3* circular transcripts, cortical and hippocampal neuron cultures were irradiated at DIV1 with 1 Gy of X-rays and RNA extracted 6 h post-irradiation for qRT-PCR. Both in cortical and hippocampal neuron cultures, several circRNAs of *Pvt1* as well as of *Ano3* were found to be significantly up-regulated after irradiation (**Figure 22**), although in general to a lesser extent as compared to the linear radiation-responsive mRNAs.

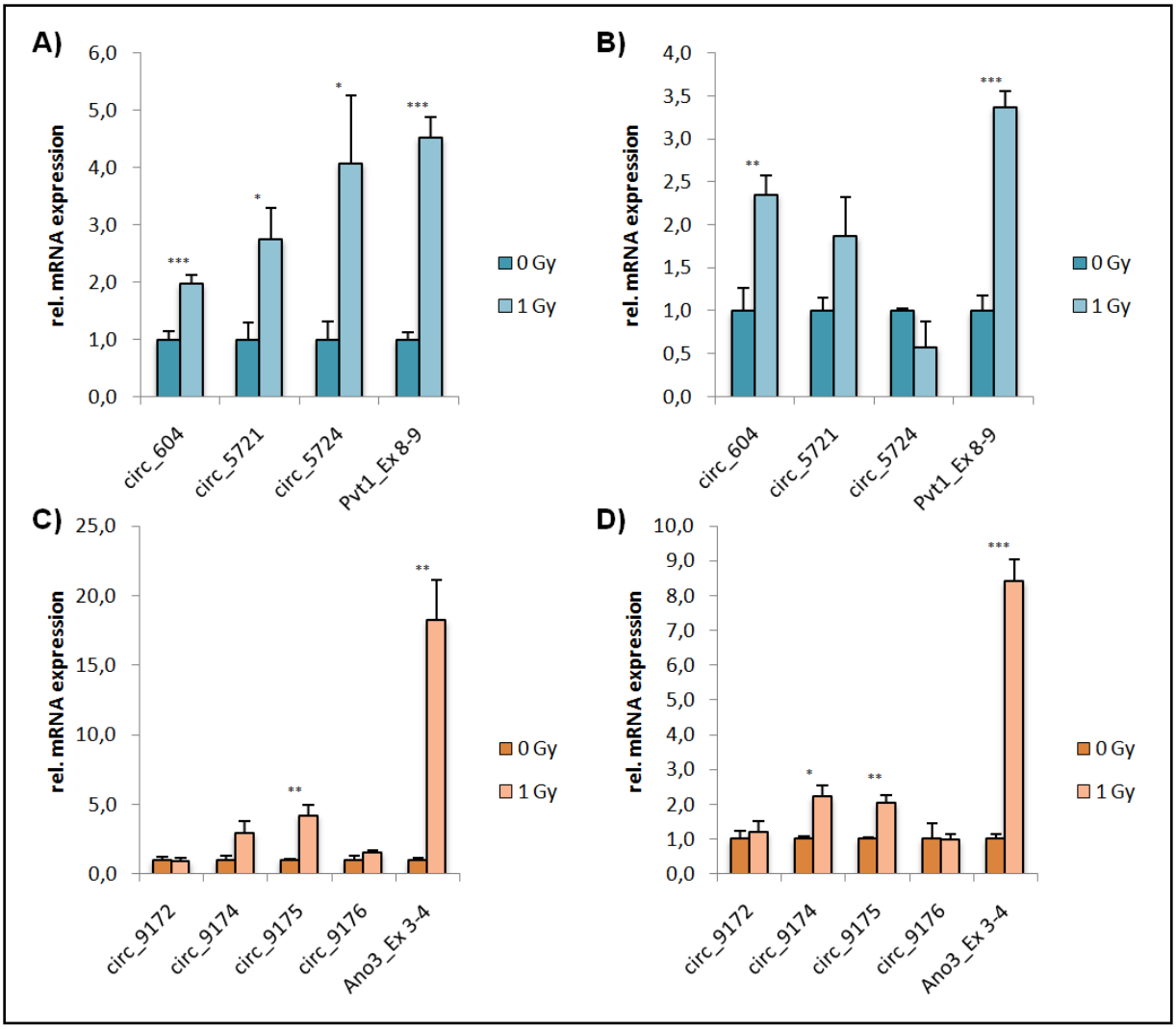

Figure 22. Expression-change of *Pvt1* transcripts after irradiation of *in vitro* cortical and hippocampal neurons. Irradiated (1Gy) and non-irradiated (0Gy) cortical (**A, C**) and hippocampal (**B, D**) neuron cultures were assessed by qRT-PCR and the changes in expression of the different *Pvt1* (**A, B**) and *Ano3* (**C, D**) transcripts were compared. Data shown are means of four replicates and the error bars indicate standard errors. *p<0.05; **p<0.01; ***p<0.001 (Student's t-test).

4.7. Circular variants of *Pvt1* and *Ano3* were not radiation-induced *in vivo*

In order to assess alterations in expression levels following radiation *in vivo*, *in utero* irradiated (1 Gy) and non-irradiated (0 Gy) E11 mice's brains were taken for RNA extraction and qRT-PCR was performed. As expected, expression of linear mRNAs of *Pvt1* and *Ano3* was clearly induced after irradiation, while all the circular RNAs failed to show any significant up-regulation (**Figure 23**).

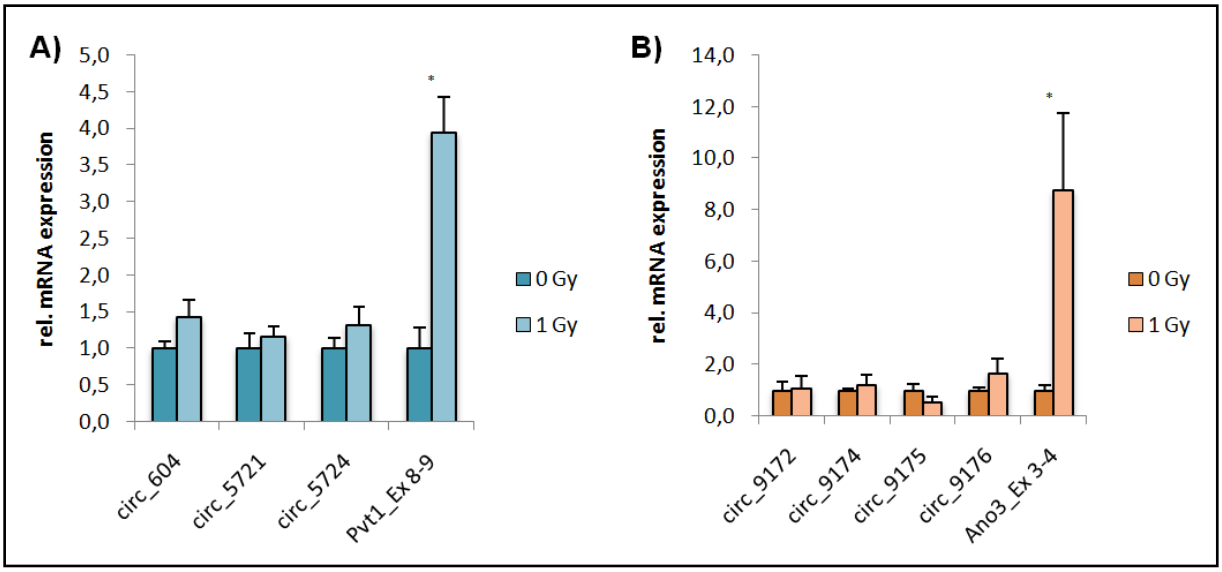

Figure 23. Up-regulation of expression after *in vivo* irradiation was limited to linear *Pvt1* and *Ano3* transcripts. Irradiated (1Gy) and non-irradiated (0Gy) brains were taken for RNA extraction and expression of the *Pvt1* (**A**) and *Ano3* (**B**) variants were assessed by qRT-PCR. Data shown are means of four replicates and the error bars indicate standard errors. *p<0.05; **p<0.01; ***p<0.001 (Student's t-test).

4.8. Potential target miRNAs are coexpressed with their targeting circRNAs in maturing primary neurons

The involvement of circRNAs as miRNA-sponges is one of its main functions that has been clearly proven until now. As an approach to identify the functional roles of our circRNAs of interest, a computational analysis was performed, searching for possible binding sites for miRNAs within our circRNAs. The hit-list that the search produced suggested that our circRNAs contained binding sites for several miRNAs. Especially for circ_5721, the largest circRNA expressed from the *Pvt1* gene, several miRNAs were found with more than one binding site, miR-705 being one of them. Also, for the linear transcript of *PVT1*, the miRNA family miR-200 had been already suggested to be a sponging target in humans[114].

In cortical neuron cultures, a dynamic up-regulation of the linear *Pvt1* transcript and circ_5721 had primarily been observed from DIV1 to DIV7 of neuronal maturation (**Figure 20A**). So, total RNA, including miRNAs, was extracted from primary cortical neuron cell cultures on DIV1, 3 and 7 which subsequently was used for qRT-PCR. Expression of miR-200 and miR-705 during neuronal maturation was then assessed. Both miRNAs exhibited up-regulated expression during differentiation (**Figure 24B, D)**, similar to the expression patterns of the respective *Pvt1* transcripts that could possibly be their sponges (**Figure 24A, C**).

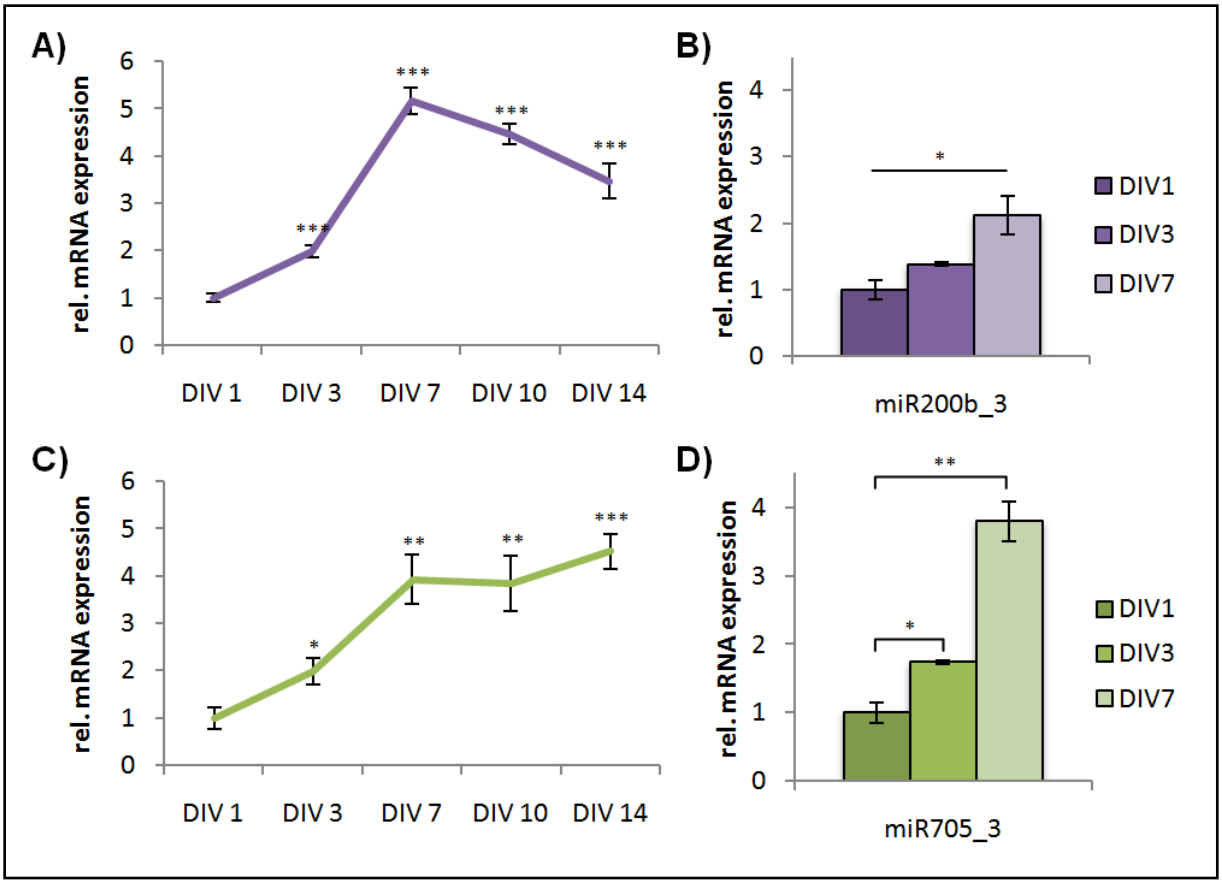

Figure 24. Expression of selected *Pvt1* transcripts during neuronal differentiation in comparison to their predicted miRNA targets. Expression-patterns of *Pvt1*-transcripts "Pvt1_Ex 8-9" (linear) (**A**) and "circ_5721" (circular) (**C**) during neuronal maturation are represented here by the line charts. The charts on the right panel show relative expressions of the predicted targets of the *Pvt1*-transcripts, miR-200 (**B**) and miR-705 (**D**) during neuronal maturation at DIV1, 3 and 7. Data shown are means of four replicates and the error bars indicate standard errors. DIV: days *in vitro*. *p<0.05; **p<0.01; ***p<0.001 (Student's t-test).

5. Discussion

5.1. Successful validation of *Pvt1*'s and *Ano3*'s circular RNAs

Thanks to the recently published immense amount of new data concerning circular RNAs, freely accessible in the public database circbase.org[115], we were able to identify several genes among the previously identified radiation-responsive genes[4] that are predicted to produce circular RNA transcripts. In this study, we successfully validated the existence and circularity of three *Pvt1*-circRNAs and four *Ano3*-circRNAs.

Based on the assumption that only RNA containing scrambled exon junctions will be able to produce PCR-products when divergent primers are used, our outwards facing primers led to successful amplification for several of the predicted circRNAs. The necessity of additional experimental verification of these circRNAs results from the fact that the scrambled exon junctions' generation is not an exclusive product of blacksplicing events.

RNaseR treatment prior to qRT-PCR allowed the enrichment of circular transcripts only, almost completely degrading linear RNAs, ensuring the replication of only circular transcripts. Little residues after RNaseR treatment may be explained by digestion that was not 100% efficient. Apparently, the degradation of the linear transcripts also led to more frequent bindings of the random primers to the circRNAs, leading to noticeably increased amplifications of the circRNAs with higher RNaseR concentrations. An additional proof for the circularity was provided by comparing PCR signals after cDNA synthesis using either random primers, which can bind both circular and linear transcripts, or oligo-dT primers, which can not bind circRNAs because they lack a poly-A tail. In comparison, the usage of random primers instead, did not make a difference at all between the circular and linear transcripts. The small amount of amplification observed for *Ano3*-circRNAs when oligo-dT primers were used for reverse transcription may be explained by unspecific binding of the oligo-dT primers on adenine rich regions of the circular transcripts. Looking into the sequences, we found that circ_9174 indeed has less adenine-rich regions than circ_9172, circ_9175 and circ_9176, which corresponds with our observations from the qRT-PCRs using oligo dT primers, where circ_9174 showed almost no expression at all and the other circRNAs still produced some residue-amplification. Surprisingly, the linear transcript of *Pvt1* generated a 6-fold increased PCR-signal when using oligo-dT primers for qRT-PCR. In contrast, the linear *Ano3*-transcript showed a lower signal after oligo-dT priming than when random primers were used. An explanation to this may be the higher reverse transcription efficiency that can be achieved when the designed qPCR primers are positioned more to the 3' end of the transcript, which is the case for Pvt1_Ex 8-9, while for Ano3_Ex 3-4 the primers are more to the 5' end that might result in lower efficiency of the reverse transcription reaction.

All results in accordance prove with certainty the circularity of the predicted circular transcripts. Also, in agreement with the theory that circular RNAs are very stable due to its inaccessibility for exonucleases[7], it was shown that all the circular transcripts are relatively stable, at least for the first 24 hours after expression. For *Ano3*, it was clearly the case that

the circular transcripts were more stable than their linear counterpart, highlighting this feature of the circRNAs. In fact, very little is known about the degradation process of circRNAs, which leaves us another question that has to be further investigated on.

5.2. circRNAs important for brain development and neuronal maturation?

Even though several updates have been published recently concerning the physiological role of circRNAs, the function of a large majority of circRNAs still remains unknown. In general, our results show an increased expression of all *Pvt1* and *Ano3* transcripts during brain development and neuronal maturation.

A deeper involvement of the circular *Pvt1* transcripts than of the linear ones later on in neuronal maturation may be speculated, since the expression of the linear *Pvt1* peaked at DIV7 and then decreased again, while expression levels of circular transcripts kept increasing until after DIV14. Supporting this theory, also *in vivo* experiments revealed similar behavior of the *Pvt1* RNAs during brain development showing a decline in linear mRNA expression after P10, while the circular transcripts further increased.

Until now, no specific function of *Pvt1* in the brain or neurons has ever been described. Therefore, the observed more steady and durable induction of the circular *Pvt1* transcripts is particularly suggestive of some kind of involvement of the circular RNAs in brain development. Looking at the expression pattern, we assume that the linear form of *Pvt1* might be important during (late) embryonic and early postnatal development, while the circular forms seem important not only during development but also in the adult brain. In agreement with this assumption and already published data from two previous studies[1, 107], we found that all circular transcripts of *Pvt1* were enriched in the adult brain compared to several other tissues. This enrichment was very much in contrast to the expression pattern of their linear transcript, especially that of circ_5721 of which the expression was practically absent in all other investigated tissues.

A notable difference in behavior between these two genes during neuronal maturation and brain development is that, while the *Pvt1* transcripts are perceived to be gradually up-regulated from onset of maturation/development, expression of *Ano3* transcripts seem increased at a later stage of maturation/development (DIV14/P30). This can be taken as an indication for the importance of *Ano3* in synaptogenesis, network formation and transmission of signals, which is in line with previous reports that state that *Ano3*, as member of a transmembrane protein family, is probably also involved in ion channel activities [96, 100, 116] that is essential for neuronal communication. In concordance with the observation of a general enrichment of circRNAs in the brain[1], and the fact that Ano3 had already been shown to be brain-specific[119], all Ano3 transcripts were almost exclusively expressed in the brain, as well as in the eye, to a lesser extent.

Based on these observations, we speculate that circRNAs are important for brain development and neuronal maturation. Involvement in different functions than their cognate

mRNAs could be hypothesized too due to the distinctive expression profiles of some circRNAs. All these results though still raise the question, what and how exactly the connection is between these enriched and up-regulated circRNAs to brain development and neuronal maturation.

5.3. Radiation-responsive circRNAs

Consistent with the data previously published[4], linear transcripts of *Pvt1* and *Ano3* could be shown to be responsive to radiation, exhibiting increased expression after irradiation in *in vitro* and *in vivo* experiments. Interestingly, we saw that some circular transcripts of both genes *Pvt1* and *Ano3* also show similar attributes as their linear cognates during *in vitro* irradiation experiments.

Also for the *in vivo* experiments, we observed some slight trend of up-regulated, radiation-responsive circRNAs, though not at all in a comparable dimension as the up-regulation of the linear transcripts. Here, it is important to keep in mind that we look at very homogenous cell types when performing *in vitro* experiments with primary cortical or hippocampal neurons, while the subset of brain cells we look at during *in vivo* experiments is very diverse. The less significant results from the *in vivo* experiments could be reasoned by this. Nevertheless, in these results we found the first indication that expression of circRNAs is up-regulated after irradiation. Therefore, these transcripts maybe should also be included in the radiation-responsive gene signature.

5.4. *Pvt1* transcripts and its activity as miRNA sponges

Aware of the fact that the one main function of circRNAs that has been already proven for two circRNAs[2, 3] is to act as sponges for miRNAs, we decided to look for abundant miRNA binding sites in our circular RNAs. Using data from a miRNA-database, computational analysis was performed to look for binding sites for miRNAs inside our circRNA sequences. This resulted in a hitlist that included miRNAs that have single or multiple binding sites for our circRNAs, providing a list of potential miRNA targets for our circRNAs (data not shown).

From those possible miRNA targets, some were chosen, such as miR-705 as presented here, to compare its expression pattern with that of its putative sponge, circ_5721 in this case. The miR-200, that had already been predicted to be a target of the linear *PVT1* mRNA earlier[114], was also chosen to be further investigated.

We found that both miRNAs and their respective sponges were up-regulated during neuronal maturation. Keeping in mind the results of computational analysis, this transcriptional coordination can be seen as a first hint that the prediction about the sponging activities may be true, since co-expressed genes tend to be functionally related too[120, 121]. If in future experiments further strong correlation in expression between the sponge and the target can be found over the complete maturation period, this can be taken as an indication for the sponge activity. In any case, conduction of further experiments, such as gene overexpression or silencing studies, is necessary to prove this. Also, while focusing on its

role as miRNA-sponges, we should be careful not to underestimate the spectrum of functional roles the diverse, quite significant group of circRNAs may be involved in.

6. Conclusions and Future Perspectives

In this study, we successfully validated the expression and circularity of three predicted circRNAs of *Pvt1* and four of *Ano3*, both genes of which the linear transcripts are part of the radiation-responsive gene signature[4]. Due to the low abundance of a large proportion of the circRNAs and the difficulty to separate the circRNAs from other RNA species[105], the existence of only very few circRNAs had been known until recently. Thanks to today's advanced techniques, several thousands of circRNAs have been added to the database, but mostly based on algorithms that look into RNA sequencing data. Our experimental verification of these transcripts adds to the advancement towards accomplishing a dataset that has validated and characterized information about the circRNAs.

We showed that both genes, *Pvt1* and *Ano3*, have very stable circular isoforms, which, especially in the case of *Ano3*, underlines the greater stability of the circular isoforms in comparison to their linear counterparts. Furthermore, we saw that there is an induction of the circular transcripts (of both genes) during neuronal maturation and brain development. This, together with the observed enrichment of the circular transcripts in the brain, which in the case of *Pvt1* is very much in contrast to its linear isoform, strongly suggest a relevant involvement of the circRNAs in brain function. Looking at the deviating expression profiles of the circular transcripts from their cognate mRNAs, we hypothesize that they are involved in different functions. Having already established radiation-responsive linear transcripts for both of our genes of interest, reasonable investigations were conducted that led to the first hints of radiation-responsiveness in the circular transcripts. Some significant up-regulations in expression of the circRNAs after exposure to radiation were observed during *in vitro* experiments, supplying us with more transcripts to be added to the radiation-responsive gene signature.

The abundance and evolutionary conservation of a significant number of circRNAs suggest these RNA species have relevant functional roles to play, of which only some, such as their involvement as miRNA-targeting sponges has been proven until now. As part of a preliminary functional analysis, two *Pvt1*-transcripts were concentrated on where we found specific miRNA-binding sites within them. During neuronal maturation, co-expression between both these transcripts and the respective miRNAs could be found, suggesting that these two transcripts might be actually acting as a sponge, targeting miRNAs. For sure, more investigation into this has to be done in order to really make a statement about the functionality. All *in vitro* experiments performed in this study are based on primary neuron cultures. Using more pluripotent cells instead, such as the P19 cells (mouse embryocarcinoma cell line that can be differentiated into neurons), primary neuron progenitor cells or embryonic stem cells, more insight could be gained regarding the expression during neuronal differentiation rather than the maturation-process that we looked into here. By further investigation, such as by performing overexpression and silencing experiments, potential roles of these circRNAs in different physiological processes could be studied, for

which the P19 cells also appear to be a more appropriate model compared to primary cells which are in general more difficult to transfect. Performing fluorescence *in situ* hybridization experiments, *in vitro* and *in vivo*, more information about their subcellular localization and spatiotemperal expression in the brain could be acquired. Many more functional involvements of the circRNAs are likely to be revealed with each new discovery we make.

Our results, together with recent insights from other studies that show the entanglement of the circRNAs and miRNAs with various diseases, suggest that the circRNAs could be targeted to address the diagnosis and treatment of major human diseases. For instance, overexpression of a certain circRNA could be targeted in order to silence miRNAs that are responsible for the pathogenesis of a certain disease. Even though it seems quite a stretch for now to say that the introduction of circRNAs to the field of personalized medicine is within reasonable, realizable margins, further thoughts should most definitely also be directed to that notion.

In conclusion, one can say that these validations of the circRNAs and the new findings we have made contribute to the rapid progress that is being made in expanding our understanding of the circRNAs and the human transcriptomes in general.

7. List of Abbreviations

Ad	Adult
ALARA	As low as reasonably achievable
Ano3	Anoctamin 3
ATM	Ataxia telangiectasia mutated protein
ATR	Ataxia telangiectasia and Rad3-related protein
BAX	Bcl-2-associated X protein
BRCA1	Breast cancer 1
CDK2	Cyclin-dependent kinase 2
CHEK1/2 / Chk1/2	Checkpoint kinase 1/2
circRNA	Circular RNA
d	Days
DIV1, DIV3…	Days *in vitro* 1, days *in vitro* 3…
DMSO	Dimethyl sulfoxide
DSB	Double strand breaks
E11, E12, …	Embryonic day 11, embryonic day 12, …
EtOH	Ethanol
Gapdh	Glyceraldehyde 3-phosphate dehydrogenase
Gy	Gray
h	Hours
HR	Homologous recombination
LET	Linear energy transfer
lncRNA	Long non coding RNA
LNT	Linear no-threshold
MDM2	Mouse double minute 2 homolog
miRNA	microRNA
mSv	milli sievert
NHEJ	Non-homologous end-joining
P10, P30, …	Post natal day 10, post natal day 30
Polr2a	DNA-directed RNA polymerase II subunit RPB1 gene
Pvt1	Plasmacytoma variant translocation 1
qRT-PCR	Quantitative reverse transcription polymerase chain reaction
RNaseR	Exonuclease RNase R
RNU6-2	U6 Small Nuclear RNA 2
SIR1	Silent information regulator 1
siRNA	Small interfering RNA
snoRNA	Small nucleolar RNA
Sv	Sievert
Tbp	TATA-binding protein
U	Unit

8. Bibliography

1. Rybak-Wolf A, Stottmeister C, Glazar P, et al. Circular RNAs in the Mammalian Brain Are Highly Abundant, Conserved, and Dynamically Expressed. Molecular cell 2015; 58: 870–885.

2. Hansen TB, Jensen TI, Clausen BH, et al. Natural RNA circles function as efficient microRNA sponges. Nature 2013; 495: 384–388.

3. Memczak S, Jens M, Elefsinioti A, et al. Circular RNAs are a large class of animal RNAs with regulatory potency. Nature 2013; 495: 333–338.

4. Quintens R, Verreet T, Janssen A, et al. Identification of novel radiation-induced p53-dependent transcripts extensively regulated during mouse brain development. Biology open 2015; 4: 331–344.

5. Stiles J and Jernigan TL. The Basics of Brain Development. Neuropsychology Review 2010; 20: 327–348.

6. Schacter D, Gilbert D, Wegner D and Hood B. Psychology: Second European Edition: Palgrave Macmillan, 2015.

7. Lasda E and Parker R. Circular RNAs: diversity of form and function. RNA (New York, N.Y.) 2014; 20: 1829–1842.

8. Lewis T. Human Brain: Facts, Anatomy & Mapping Project, http://www.live science.com/29365-human-brain.html (accessed 20 January 2016).

9. ASU - Ask A Biologist. Brain Regions and Functions, https://ask abiologist.asu.edu/what-your-brain-doing (2011, accessed 20 January 2016).

10. Jiang X and Nardelli J. Cellular and molecular introduction to brain development. Neurobiology of disease 2015.

11. Ronan JL, Wu W and Crabtree GR. From neural development to cognition: unexpected roles for chromatin. Nature Reviews Genetics 2013; 14: 347–359.

12. Wikipedia Contributors. Neural development, https://en.wikipedia.org/wiki/Neural_development (2015, accessed 20 January 2016).

13. Australian Government, ARPANSA. Radiation Protection, Introduction to Radiation Basics: Gamma Radiation, http://www.arpansa.gov.au/radiationprotection/basics/ gamma.cfm (2012, accessed 13 January 2016).

14. Kolb B and Gibb R. Brain Plasticity and Behaviour in the Developing Brain. Journal of the Canadian Academy of Child and Adolescent Psychiatry 2011; 20: 265–276.

15. Spalding KL, Bergmann O, Alkass K, et al. Dynamics of hippocampal neurogenesis in adult humans. Cell 2013; 153: 1219–1227.

16. Ivancevic VG and Ivancevic TT. Quantum Neural Computation: Springer Netherlands, 2010.

17. Sun T and Hevner RF. Growth and folding of the mammalian cerebral cortex: from molecules to malformations. Nature reviews. Neuroscience 2014; 15: 217–232.

18. Kowalczyk T, Pontious A, Englund C, et al. Intermediate neuronal progenitors (basal progenitors) produce pyramidal-projection neurons for all layers of cerebral cortex. Cerebral cortex (New York, N.Y. 1991) 2009; 19: 2439–2450.

19. Götz M and Huttner WB. The cell biology of neurogenesis. Nature Reviews Molecular Cell Biology 2005; 6: 777–788.

20. Verreet T et al. unpublished results.

21. Azzarelli R, Guillemot F and Pacary E. Function and regulation of Rnd proteins in cortical projection neuron migration. Frontiers in Neuroscience 2015; 9: 19, http://journal.frontiersin.org/article/10.3389/fnins.2015.00019/full (2015).

22. Van den Ameele J, Tiberi L, Vanderhaeghen P and Espuny-Camacho I. Thinking out of the dish: what to learn about cortical development using pluripotent stem cells. Trends in Neurosciences 2014; 37: 334–342, http://www.cell.com/article/S0166223614000447/fulltext (2014).

23. Suresh Parmar. How many layers of neurons are there in the human brain? , https://www.quora.com/How-many-layers-of-neurons-are-there-in-the-human-brain (2015, accessed 28 May 2016).

24. Molyneaux BJ, Arlotta P, Menezes JRL and MacKlis JD. Neuronal subtype specification in the cerebral cortex. Nature Reviews Neuroscience 2007; 8: 427–437.

25. Greig LC, Woodworth MB, Galazo MJ, Padmanabhan H and MacKlis JD. Molecular logic of neocortical projection neuron specification, development and diversity. Nature Reviews Neuroscience 2013; 14: 755–769.

26. Gupta A, Tsai L and Wynshaw-Boris A. Life is a journey: a genetic look at neocortical development. Nature reviews. Genetics 2002; 3: 342–355.

27. Hart S. Ionising radiation: promoting safety for patients, visitors and staff. Nursing standard (Royal College of Nursing (Great Britain) 1987) 2006; 20: 47-57; quiz 58, 60.

28. Wei H and Kwan NY. Advances in Biomedical Sciences and Engineering: Chapter 6, Response of Cells to Ionizing Radiation - Pp. 204-262 (59). Hong Kong: Bentham Science Publishers Ltd., 2010.

29. International Atomic Energy Agency. Radiation Biology: A Handbook for Teachers and Students. Vienna: Sales and Promotion, Publishing Section, International Atomic Energy Agency, 2010.

30. Mustafa Gök, Murat Bozkurt, Serkan Guneyli, Duygu Kara Bozkurt, Mehmet Korkmaz, Nuri Peker. Prenatal Radiation Exposure. Proceedings in Obstetrics and Gynecology 2015: 5(1): Article 2 [10 p.], http://ir.uiowa.edu/pog_in_press/ (2015, accessed 13 January 2016).

31. Nagalingam Suntharalingam, Ervin B. Podgorsak, Jolyon H. Hendry. Review of Radiation Oncology Physics: A Handbook for Teachers and Students: Chapter 14., Basic Radiobiology.

32. The University of Arizona. Radioactive Material Protection: Reference Guide. Tucson, AZ 85724, 2008.

33. EPA. Radiation: Facts, Risks and Realities: Radiation Basics, http://www.epa.gov/radiation/radiation-basics#tab-2 (2012, accessed 13 January 2016).

34. Baes F. What Types of Radiation Are There?, http://hps.org/publicinformation/ate/faqs/radiationtypes.html (2015, accessed 8 December 2015).

35. Cyberphysics - Electromagnetic Spectrum: a web-based teaching aid - for students of physics, their teachers and parents…, http://www.cyberphysics.co.uk/topics/light/emspect.htm (2016, accessed 13 January 2016).

36. United States Environmental Protection Agency. Ionizing Radiation: Fact Book, 2007.

37. MIT Massachusetts Institute of Technology. Introduction to Ionizing Radiation: Adsorbed Dose, 2006.

38. Albert C. Thompson and Douglas Vaughan (ed). X-Ray Data Booklet: RADIOACTIVITY AND RADIATION PROTECTION. 2nd edition. Berkeley, California, 2001.

39. Wikipedia Contributors. Sievert, https://en.wikipedia.org/wiki/Sievert (2016, accessed 13 January 2016).

40. Australian Government, ARPANSA. Radiation Protection, Radiation and Health Fact Sheets: Ionising Radiation and Health, http://www.arpansa.gov.au/radiationprotection/Factsheets/is_ionising.cfm (2015, accessed 13 January 2016).

41. Little MP. A Review of Non-Cancer Effects, Especially Circulatory and Ocular Diseases1. Radiation and environmental biophysics 2013; 52: 435–449.

42. Hong Kong Observatory, The Government of Hong Kong Special Administrative Region. Radiation and Health: What are the biological effects of ionizing radiation?, http://www.hko.gov.hk/education/dbcp/rad_health/eng/r4_1.htm (2012, accessed 13 January 2016).

43. Tore Straume, Steve Blattnig and Cary Zeitlin. Radiation Hazards and the Colonization of Mars:Brain, Body, Pregnancy, In-Utero Development, Cardio, Cancer,

Degeneration. Journal of Cosmology 2010; 12: 3992–4033, http://journalofcosmology.com/Mars124.html (2010, accessed 14 January 2016).

44. Doss M. Linear No-Threshold Model VS. Radiation Hormesis. Dose-Response 2013; 11: 495–512.

45. Canadian Nuclear Safety Commission. Linear-Non-Threshold Model, http://nuclearsafety.gc.ca/eng/resources/health/linear-non-threshold-model/index.cfm (2013, accessed 14 January 2016).

46. Tubiana M, Feinendegen LE, Yang C and Kaminski JM. The Linear No-Threshold Relationship Is Inconsistent with Radiation Biologic and Experimental Data. Radiology 2009; 251: 13–22.

47. Wodarz D, Sorace R and Komarova NL. Dynamics of Cellular Responses to Radiation. PLoS Computational Biology 2014; 10.

48. Robertson A, Allen J, Laney R and Curnow A. The Cellular and Molecular Carcinogenic Effects of Radon Exposure: A Review. International Journal of Molecular Sciences 2013; 14: 14024–14063, http://www.mdpi.com/1422-0067/14/7/14024/pdf (2013).

49. Minafra L and Bravatà V. Cell and molecular response to IORT treatment. Translational Cancer Research 2014; 3: 32–47.

50. E. B. Podgorsak. Radiation Oncology Physics: A Handbook for Teachers and Students. Vienna, 2005.

51. Lohrer HD, Hieber L and Zitzelsberger H. Differential mutation frequency in mitochondrial DNA from thyroid tumours. Carcinogenesis 2002; 23: 1577–1582, http://carcin.oxfordjournals.org/content/23/10/1577.full (2002).

52. Alexeyev M, Shokolenko I, Wilson G and Ledoux S. The Maintenance of Mitochondrial DNA Integrity—Critical Analysis and Update. Cold Spring Harbor Perspectives in Biology 2013; 5: a012641, http://cshperspectives.cshlp.org/content/5/5/a012641.full (2013).

53. Azzam EI, Jay-Gerin J and Pain D. Ionizing radiation-induced metabolic oxidative stress and prolonged cell injury. Cancer letters 2012; 327: 48–60.

54. Stickel S, Gomes N and Su TT. The Role of Translational Regulation in Survival after Radiation Damage; an Opportunity for Proteomics Analysis. Proteomes 2014; 2: 272–290, http://www.mdpi.com/2227-7382/2/2/272/pdf (2014).

55. Brissett NC, Martin MJ, Bartlett EJ, Bianchi J, Blanco L and Doherty AJ. Molecular Basis for DNA Double-Strand Break Annealing and Primer Extension by an NHEJ DNA Polymerase. Cell Reports 2013; 5: 1108–1120, http://www.cell.com/article/S2211124713006001/fulltext (2013).

56. Halimi M, Asghari SM, Sariri R, Moslemi D and Parsian H. Cellular Response to Ionizing Radiation: A MicroRNA Story. International Journal of Molecular and Cellular Medicine 2012; 1: 178–184.

57. Staveley BE. Principles of Cell Biology (BIOL2060): The Cell Cycle: DNA replication and mitosis, http://www.mun.ca/biology/desmid/brian/BIOL2060/BIOL2060-19/CB19.html (accessed 18 January 2016).

58. Fei P and El-Deiry WS. P53 and radiation responses. Oncogene 2003; 22: 5774–5783.

59. Amestoy W. Review of Medical Dosimetry: A Study Guide: Springer International Publishing, 2015.

60. Yasuda T, Kimori Y, Nagata K, et al. Irradiation-injured brain tissues can self-renew in the absence of the pivotal tumor suppressor p53 in the medaka (Oryzias latipes) embryo. Journal of Radiation Research 2016; 57: 9–15.

61. Pao GM, Zhu Q, Perez-Garcia CG, et al. Role of BRCA1 in brain development. Proceedings of the National Academy of Sciences of the United States of America 2014; 111: E1240-8.

62. Budanov AV. The role of tumor suppressor p53 in the antioxidant defense and metabolism. Sub-cellular biochemistry 2014; 85: 337–358.

63. Zio D de, Cianfanelli V and Cecconi F. New Insights into the Link Between DNA Damage and Apoptosis. Antioxidants & Redox Signaling 2013; 19: 559–571.

64. Chang JR, Ghafouri M, Mukerjee R, Bagashev A, Chabrashvili T and Sawaya BE. Role of p53 in Neurodegenerative Diseases. Neuro-Degenerative Diseases 2012; 9: 68–80.

65. Chene P. Inhibiting the p53-MDM2 interaction: an important target for cancer therapy. Nature reviews. Cancer 2003; 3: 102–109.

66. Jayadev S, Yun B, Nguyen H, Yokoo H, Morrison RS and Garden GA. The glial response to CNS HIV infection includes p53 activation and increased expression of p53 target genes. Journal of neuroimmune pharmacology the official journal of the Society on NeuroImmune Pharmacology 2007; 2: 359–370.

67. Proctor CJ and Gray DA. GSK3 and p53 - is there a link in Alzheimer's disease? Molecular neurodegeneration 2010; 5: 7.

68. Eun B, Cho B, Moon Y, et al. Induction of neuronal apoptosis by expression of Hes6 via p53-dependent pathway. Brain research 2010; 1313: 1–8.

69. Tedeschi A and Di Giovanni S. The non-apoptotic role of p53 in neuronal biology: enlightening the dark side of the moon. EMBO Reports 2009; 10: 576–583.

70. Di Giovanni S and Rathore K. p53-Dependent pathways in neurite outgrowth and axonal regeneration. Cell and tissue research 2012; 349: 87–95.

71. Liu B, Bhatt D, Oltvai ZN, Greenberger JS and Bahar I. Significance of p53 dynamics in regulating apoptosis in response to ionizing radiation, and polypharmacological strategies. Scientific Reports 2014; 4: 6245, http://www.nature.com/srep/2014/140901/srep06245/full/srep06245.html (2014).

72. Sakamoto-Hojo ET, Mello SS, Pereira E, et al. Gene expression profiles in human cells submitted to genotoxic stress. Mutation research 2003; 544: 403–413.

73. Coleman MA, Yin E, Peterson LE, et al. Low-dose irradiation alters the transcript profiles of human lymphoblastoid cells including genes associated with cytogenetic radioadaptive response. Radiation research 2005; 164: 369–382.

74. Zhao Y, Zhong R, Sun L, Jia J, Ma S and Liu X. Ionizing Radiation-Induced Adaptive Response in Fibroblasts under Both Monolayer and 3-Dimensional Conditions. PLoS ONE 2015; 10.

75. Valentin J. Biological effects after prenatal irradiation (embryo and fetus). Annals of the ICRP 2003; 33: 1–206.

76. Radiation C, Sciences CL, Studies D and Council NR. Health Effects of Exposure to Low Levels of Ionizing Radiation: BEIR V: National Academies Press, 1990.

77. Otake M and Schull WJ. Radiation-related brain damage and growth retardation among the prenatally exposed atomic bomb survivors. International journal of radiation biology 1998; 74: 159–171.

78. Friedman HR and Selemon LD. Fetal Irradiation Interferes with Adult Cognition in the Nonhuman Primate. Biological psychiatry 2010; 68: 108–111.

79. Algan O and Rakic P. Radiation-induced, lamina-specific deletion of neurons in the primate visual cortex. The Journal of comparative neurology 1997; 381: 335–352.

80. Schmidt SL and Lent R. Effects of prenatal irradiation on the development of cerebral cortex and corpus callosum of the mouse. The Journal of comparative neurology 1987; 264: 193–204.

81. Verreet T, Quintens R, van Dam D, et al. A multidisciplinary approach unravels early and persistent effects of X-ray exposure at the onset of prenatal neurogenesis. Journal of Neurodevelopmental Disorders 2015; 7.

82. Ishida Y, Ohmachi Y, Takai N, et al. Neurobehavioral changes in mice exposed to fast neutrons in utero. Journal of radiation research 2011; 52: 257–263.

83. Takata H, Hanafusa T, Mori T, et al. Chromatin Compaction Protects Genomic DNA from Radiation Damage. PLOS ONE 2013; 8: e75622, http://journals.plos.org/plosone/article/asset?id=10.1371/journal.pone.0075622.PDF (2013).

84. Vogin G and Foray N. The law of Bergonié and Tribondeau: a nice formula for a first approximation. International journal of radiation biology 2013; 89: 2–8.

85. Picano E, Vano E, Domenici L, Bottai M and Thierry-Chef I. Cancer and non-cancer brain and eye effects of chronic low-dose ionizing radiation exposure. BMC Cancer 2012; 12: 157.

86. Cryan JF and Holmes A. The ascent of mouse: advances in modelling human depression and anxiety. Nature reviews. Drug discovery 2005; 4: 775–790.

87. Lui JH, Hansen DV and Kriegstein AR. Development and evolution of the human neocortex. Cell 2011; 146: 18–36.

88. Shepherd GM. The Microcircuit Concept Applied to Cortical Evolution: from Three-Layer to Six-Layer Cortex. Frontiers in Neuroanatomy 2011; 5.

89. Barton RA and Harvey PH. Mosaic evolution of brain structure in mammals. Nature 2000; 405: 1055–1058.

90. Semple BD, Blomgren K, Gimlin K, Ferriero DM and Noble-Haeusslein LJ. Brain development in rodents and humans: Identifying benchmarks of maturation and vulnerability to injury across species. Progress in neurobiology 2013; 0: 1–16.

91. Miller JA, Ding S, Sunkin SM, et al. Transcriptional landscape of the prenatal human brain. Nature 2014; 508: 199–206.

92. Chou S, Wang C, Sintupisut N, et al. Analysis of spatial-temporal gene expression patterns reveals dynamics and regionalization in developing mouse brain. Scientific Reports 2016; 6: 19274.

93. Pollock A, Bian S, Zhang C, Chen Z and Sun T. Growth of the developing cerebral cortex is controlled by microRNA miR-7 through modifying the p53 pathway. Cell reports 2014; 7: 1184–1196.

94. Silver DL, Watkins-Chow DE, Schreck KC, et al. The exon junction complex component Magoh controls brain size by regulating neural stem cell division. Nature neuroscience 2010; 13: 551–558.

95. Colombo T, Farina L, Macino G and Paci P. PVT1: a rising star among oncogenic long noncoding RNAs. BioMed research international 2015; 2015: 304208.

96. Charlesworth G, Bhatia KP and Wood NW. The genetics of dystonia: new twists in an old tale. Brain a journal of neurology 2013; 136: 2017–2037.

97. Pedemonte N and Galietta LJV. Structure and function of TMEM16 proteins (anoctamins). Physiological reviews 2014; 94: 419–459.

98. Charlesworth G, Plagnol V, Holmström KM, et al. Mutations in ANO3 cause dominant craniocervical dystonia: ion channel implicated in pathogenesis. American journal of human genetics 2012; 91: 1041–1050.

99. Briones N and Dinu V. Data mining of high density genomic variant data for prediction of Alzheimer's disease risk. BMC medical genetics 2012; 13: 7.

100. Huang F, Wang X, Ostertag EM, et al. TMEM16C facilitates Na+-activated K+ currents in rat sensory neurons and regulates pain processing. Nature neuroscience 2013; 16: 1284–1290.

101. Guo JU, Agarwal V, Guo H and Bartel DP. Expanded identification and characterization of mammalian circular RNAs. Genome biology 2014; 15: 409.

102. Bachmayr-Heyda A, Reiner AT, Auer K, et al. Correlation of circular RNA abundance with proliferation--exemplified with colorectal and ovarian cancer, idiopathic lung fibrosis, and normal human tissues. Scientific Reports 2015; 5: 8057.

103. Huang C and Shan G. What happens at or after transcription: Insights into circRNA biogenesis and function. Transcription 2015; 6: 61–64.

104. Jeck WR, Sorrentino JA, Wang K, et al. Circular RNAs are abundant, conserved, and associated with ALU repeats. RNA 2013; 19: 141–157.

105. Jeck WR and Sharpless NE. Detecting and characterizing circular RNAs. Nature Biotechnology 2014; 32: 453–461.

106. Copyright: Roel Quintens

107. You X, Vlatkovic I, Babic A, et al. Neural circular RNAs are derived from synaptic genes and regulated by development and plasticity. Nature neuroscience 2015; 18: 603–610.

108. Wikipedia Contributors. Forebrain, https://en.wikipedia.org/wiki/Forebrain (2015, accessed 20 January 2016).

109. Qu S, Yang X, Li X, et al. Circular RNA: A new star of noncoding RNAs. Cancer letters 2015; 365: 141–148.

110. Guil S and Esteller M. RNA-RNA interactions in gene regulation: the coding and noncoding players. Trends in biochemical sciences 2015; 40: 248–256.

111. Hentze MW and Preiss T. Circular RNAs: splicing's enigma variations. The EMBO Journal 2013; 32: 923–925.

112. Benotmane M. Non-conventional apoptotic response to ionising radiation mediated by N-methyl D-aspartate receptors in immature neuronal cells. International Journal of Molecular Medicine 2013.

113. Pfaffl MW. A new mathematical model for relative quantification in real-time RT–PCR. Nucleic Acids Research 2001; 29: e45.

114. Paci P, Colombo T and Farina L. Computational analysis identifies a sponge interaction network between long non-coding RNAs and messenger RNAs in human breast cancer. BMC systems biology 2014; 8: 83.

115. Glažar P, Papavasileiou P and Rajewsky N. circBase: a database for circular RNAs. RNA (New York, N.Y.) 2014; 20: 1666–1670.

116. Feenstra B, Pasternak B, Geller F, et al. Common variants associated with general and MMR vaccine-related febrile seizures. Nature genetics 2014; 46: 1274–1282.

117. Wikipedia Contributors. Human brain, https://en.wikipedia.org/wiki/Human_brain (2016, accessed 20 January 2016).

118. Verreet T, Rangarajan JR, Quintens R, et al. Persistent Impact of In utero Irradiation on Mouse Brain Structure and Function Characterized by MR Imaging and Behavioral Analysis. Frontiers in behavioral neuroscience 2016; 10: 83.

119. Suzuki J, Fujii T, Imao T, Ishihara K, Kuba H and Nagata S. Calcium-dependent Phospholipid Scramblase Activity of TMEM16 Protein Family Members*. The Journal of Biological Chemistry 2013; 288: 13305–13316.

120. Heyer LJ. Exploring Expression Data: Identification and Analysis of Coexpressed Genes. *Genome Research* 1999; 9: 1106–1115

121. Hsu C, Juan H and Huang H. Functional Analysis and Characterization of Differential Coexpression Networks. *Scientific Reports* 2015; 5: 13295, http://www.nature.com/srep/2015/150818/srep13295/full/srep13295.html (2015).

9. Annex

Linear and circular transcripts of *Pvt1* is induced during neuronal maturation in primary hippocampal neurons

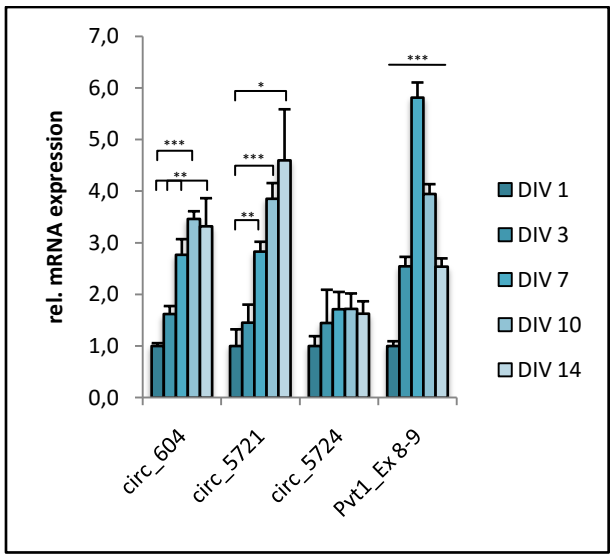

Figure I. Induction of *Pvt1* transcripts during neuronal maturation. Relative expression of linear and circular *Pvt1* transcripts during hippocampal neuron maturation is shown here. Data shown are means of four replicates and the indicated error bars represent standard errors. DIV: days *in vitro.* *p<0.05; **p<0.01; ***p<0.001 (Student's t-test).